The Journal of Neuroscience, August 1990, 10(8): 2560–2579

Different Cellular Types in Mesopontine Cholinergic Nuclei Related to Ponto-Geniculo-Occipital Waves

M. Steriade, D. Paré, S. Datta, G. Oakson, and R. Curró Dossi

Laboratoire de Neurophysiologie, Faculté de Médecine, Université Laval, Québec, Canada G1K 7P4

The only mesopontine neurons previously described as involved in the transfer of ponto-geniculo-occipital (PGO) waves from the brain stem to the thalamus were termed PGO-on bursting cells. We have studied, in chronically implanted cats, neuronal activities in brain-stem peribrachial (PB) and laterodorsal tegmental (LDT) cholinergic nuclei in relation to PGO waves recorded from the lateral geniculate (LG) thalamic nucleus during rapid-eye-movement (REM) sleep. We constructed peri-PGO histograms of PB/LDT cells' discharges and analyzed the interspike interval distribution during the period of increased neuronal activity related to PGO waves.

Six categories of PGO-related PB/LDT neurons with identified thalamic projections were found: 4 classes of PGO-on cells; PGO-off but REM-on cells; and post-PGO cells. The physiological characteristics of a given cell class were stable even during prolonged recordings. One of these cell classes (1) represents the previously described PGO-on bursting neurons, while the other five (2–6) are newly discovered neuronal types. (1) Some neurons (16% of PGO-related cells) discharged stereotyped low-frequency (120–180 Hz) spike bursts preceding the negative peak of the LG-PGO waves by 20–40 msec. These neurons had low firing rates (0.5–3.5 Hz) during all states. (2) A distinct cell class (22% of PGO-related neurons) fired high-frequency spike bursts (>500 Hz) about 20–40 msec prior to the thalamic PGO wave. These bursts were preceded by a period (150–200 msec) of discharge acceleration on a background of tonically increased activity during REM sleep. (3) PGO-on tonic neurons (20% of PGO-related neurons) discharged trains of repetitive single spikes preceding the thalamic PGO waves by 100–150 msec, but never fired high-frequency spike bursts. (4) Other PGO-on neurons (10% of PGO-related neurons) discharged single spikes preceding thalamic PGO waves by 15–30 msec. On the basis of parallel intracellular recordings in acutely prepared, reserpine-treated animals, we concluded that the PGO-on single spikes arise from conventional excitatory postsynaptic potentials and do not reflect tiny postinhibitory rebounds. (5) A peculiar cellular class, termed PGO-off elements (8% of PGO-related neurons), consisted of neurons with tonic, high discharge rates (>30 Hz) during REM sleep. These neurons stopped firing 100–200 msec before and during the thalamic PGO waves. (6) Finally, other neurons discharged spike bursts or tonic spike trains 100–300 msec after the initially negative peak of the thalamic PGO field potential (post-PGO elements, 23% of PGO-related neurons). With the exception of low-frequency bursting neurons, all other cell types are part of the fast-discharging cell group reported in the companion paper.

The comparison between the firing patterns of various PGO-on neurons and the ionic conductances generating the electroresponsiveness of various brain-stem reticular cell classes studied *in vitro* allowed inferences to be drawn concerning the intrinsic PB/LDT circuitry and its extrinsic modulation. The excitatory and inhibitory inputs acting on PB/LDT cells create the necessary background for low-threshold rebound bursts, high-threshold spike bursts, and PGO-on tonic discharges. The PGO-off neurons are hypothesized to reflect activities in local GABAergic neurons whose silent firing during PGO waves would disinhibit adjacent PGO-on neurons.

Ponto-geniculo-occipital (PGO) waves herald the state of rapid-eye-movement (REM) sleep and continue throughout it. PGO waves are regarded as a physiological correlate of the hallucinoid imagery during dreaming mentation. Several lines of evidence suggest that brain-stem peribrachial (PB) and laterodorsal tegmental (LDT) neurons are the final common path for the transfer of PGO signals to thalamocortical systems. First, PB stimulation induces a sharp PGO wave in the lateral geniculate (LG) thalamic nucleus (Sakai et al., 1976). The PB-evoked thalamic PGO wave is associated with a depolarization of LG relay neurons, starting at a latency of 20–40 msec and lasting for 150–300 msec when not interrupted by an all-or-none inhibitory postsynaptic potential (IPSP) (Hu et al., 1989). Second, excitotoxic lesions of the PB/LDT area, leading to a loss of 60% of choline acetyltransferase (ChAT)-positive cells, reduce by about 75% the thalamic PGO rate during REM sleep (Webster and Jones, 1988). And third, a set of neurons recorded from the PB/LDT area, described as PGO-on burst neurons, discharge a group of 2–6 spikes preceding the LG-PGO wave by about 10–20 msec (Saito et al., 1977; McCarley et al., 1978; Sakai and Jouvet, 1980). A 3-way correlation was found between the eye movement direction and the discharge of PB burst neurons related to the LG-PGO wave: rightward eye movements drive right PB neurons that lead to LG-PGO waves of larger amplitude on the right side (Nelson et al., 1983). The mechanism of PGO-on bursting

Received Dec. 14, 1989; revised Feb. 16, 1990; accepted Mar. 12, 1990.

This work was supported by the Medical Research Council of Canada (MT-3689). D.P. had an MRC studentship. S.D. was a postdoctoral fellow, on leave of absence from All-India Institute of Medical Sciences, New Delhi, India. R.C.D. was a postdoctoral fellow, on leave of absence from University of Padova, Italy.

cells was generally viewed as a disinhibition of mesopontine cholinergic neurons due to the cessation of firing, during REM sleep, of presumably inhibitory monoaminergic neurons (see Sakai, 1985; Callaway et al., 1987).

The earlier description of PGO-on burst neurons left open a series of questions.

1. It was reported that PGO-on burst neurons represent quite small proportions of the total number of neurons sampled in mesopontine cholinergic PB, LDT, and parabrachial nuclei: less than 10% (Sakai and Jouvet, 1980) or 5% (Nelson et al., 1983). What is the behavior of the overwhelming majority of neurons in PB and LDT nuclei in relation with thalamic PGO waves? It is believed that the thalamic PGO waves are cholinergic events mediated by nicotinic receptors, as they are blocked by systemic administration (Ruch-Monachon et al., 1976) or iontophoretic application (Hu et al., 1988) of mecamylamine. *In vitro* studies reached the conclusion that pedunculopontine neurons characterized by the property of generating low-threshold spikes (LTSs) crowned by bursts of sodium action potentials are *not* cholinergic (Kang and Kitai, 1990; Leonard and Llinás, 1990). The following question then arises: Do the bursts represent the only type of activity able to transfer the PGO signal to the thalamus?

2. Are PGO-bursting cells distinct from PB/LDT neurons discharging tonically, with high firing rates (>10 Hz) during EEG-desynchronized states of wakefulness (W) and REM sleep (Steriade et al., 1990)? In other words, are there 2 different classes of mesopontine cholinergic neurons, 1 involved in tonic ascending activation processes, the other generating the phasic thalamocortical events of REM sleep? Previous studies have emphasized that PGO-on burst neurons have low firing rates (<1.5 Hz) during quiet W and REM sleep without PGO waves (Sakai and Jouvet, 1980) and may discharge with spike bursts (Sakai and Jouvet, 1980) or single spikes (Nelson et al., 1983) in relation to eye movement potentials (EMPs) during W. A more recent study reiterated the emphasis that PGO-on burst neurons are a special cell class, as compared to other mesopontine neurons displaying tonic or phasic discharge patterns during REM sleep (El Mansari et al., 1989). These data suggest the distinctiveness of phasic (PGO- and EMP-related), as opposed to tonic, mesopontine neurons. We will show in this study that a newly discovered, thalamic-projecting neuronal type in PB/LDT nuclei displays PGO-on spike bursts on the background of tonically increased discharge rate during REM sleep and that these neurons discharge as well tonically, at high rates, during W.

3. Although disinhibition may account for the tonically increased discharge rates of PB/LDT cholinergic neurons during REM sleep, as a consequence of silenced firing in inhibitory dorsal raphe neurons (see Steriade et al., 1990), the current idea of disinhibition as an underlying mechanism of PGO-on bursts is probably not a correct interpretation. Instead, we started with the hypothesis (Steriade and Paré, 1990) that PGO-on bursts appearing on a background of neuronal silence or diminished firing rate during REM sleep are more likely generated by LTSs deinactivated by membrane hyperpolarization. LTSs have been found in some neurons of the pedunculopontine (Leonard and Llinás, 1987, 1990; Kang and Kitai, 1990) and LDT (Wilcox et al., 1989) nuclei. If so, we should examine the possibility of inhibitory processes acting on PB and LDT neurons, during which central excitatory signals may trigger LTSs.

This study describes the complex discharge patterns in various PGO-related PB/LDT cells and discusses their different generator mechanisms.

Materials and Methods

Data presented here are derived from the same chronically implanted cats reported in the accompanying paper (Steriade et al., 1990). The procedures for preparation, recording, stimulation, neuronal identification, and histological control were the same.

Analyses of PGO-related neuronal activity in PB/LDT areas. Focal PGO waves in the LG thalamic nucleus were recorded simultaneously with unit activity in the PB or LDT brain-stem areas during the transitional epoch between EEG-synchronized sleep (S) and REM sleep (termed pre-REM) and during full-blown REM sleep (see Fig. 2 in the preceding paper). Focal waves were digitized on a Data Precision model 6000 analyzer, using a signal bandwidth of 30 Hz and a sampling rate of 100 samples/sec. The time of the PGO negative peak (T_0) was determined by displaying the focal waves on a personal computer and identifying each PGO using a "mouse." The computer then searched the epoch to determine the exact time of the initially negative peak of PGO wave to an accuracy of 10 msec or 1 sampling period, and stored T_0 and the PGO peak amplitude in a table. For the same epoch, unit interspike intervals from PB or LDT neuronal activities were also measured and stored with a resolution of 100 μsec.

The time range for PGO correlations with PB or LDT unit interspike intervals was chosen to be from T_0 − 300 msec (in some cases T_0 − 600 msec) to T_0 + 300 msec. To ensure that activity in the specified time range around the PGO waves was not contaminated by effects due to adjacent PGO events, only those single PGO waves and PGO clusters that were separated by at least 600 msec (in some cases 900 msec) were selected for analysis. PGO clusters were recognized and marked as groups of 2 or more PGO waves separated by less than 300 msec. The T_0 of a PGO cluster was taken as the time of the first PGO negative peak. To retain an epoch for analysis, the epoch had to contain at least 5 analyzable PGO events.

For correlations between PGO events and PB or LDT unitary spikes, the times of single or clustered PGO waves were retrieved along with the spike firing times that fell within the time range from T_0 − 300 msec (or T_0 − 600 msec) to T_0 + 300 msec of each PGO wave. A peri-PGO spike histogram (PPSH) of all PGO events was produced to show average spike activity around T_0. For those PPSHs showing pronounced increases in activity compared to the first 100 msec (in some cases 200 msec) of the time range, the spikes occurring within the period of increased discharge were fetched and used to produce the peri-PGO interval histogram (PPIH) which gives the interspike interval distribution of the spikes participating in the PGO-related increase in neuronal activity.

The averaged PPSH ordinate was calibrated in effective unit firing rate (Hz, spikes/sec) by

$$FS = (1000 \times C)/NP \times BW,$$

where FS is equivalent unit firing rate (Hz); NP, the number of PGOs analyzed in epoch; C, total counts in bin for NP histograms; and BW, the bin width (msec). Pooled PPSHs and PPIHs for multiple cells were obtained by computing the bin-by-bin median and mean, respectively, across all histograms for all available cells in the same neuronal class.

In some neurons, PPSHs and PPIHs were analyzed together with interspike interval histograms (ISIHs) from the whole W, S, and REM states to gain information about the behavior of PGO-related neurons during all states of vigilance.

Results

Data base

We have recorded 780 cells within the limits of PB and LDT cholinergic nuclei, as recognized on NADPH-diaphorase-stained sections (see data base and Fig. 1 in Steriade et al., 1990). Upon visual inspection of polygraphic recordings, the activity of 187 units (129 PB and 58 LDT neurons) increased or, much less often, decreased in relation to LG-PGO waves during the transitional pre-REM epoch and REM sleep. All these cells were analyzed for their PPSHs (see Materials and Methods).

Eighty elements were further analyzed to determine the dis-

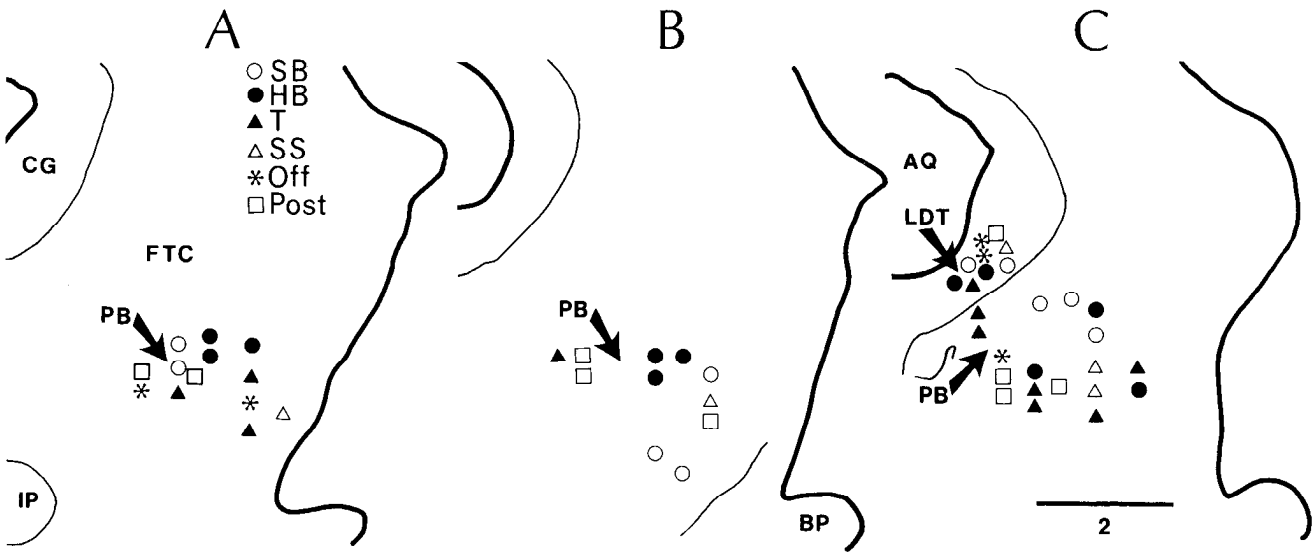

Figure 1. Brain-stem location of 51 cells related in different ways to thalamic PGO waves. *A–C,* Three levels (stereotaxic planes A1–P1). Symbols in *A*: *SB,* PGO-on sluggish-burst neurons; *HB,* PGO-on high-frequency burst neurons; *T,* PGO-on tonic neurons; *SS,* PGO-on single-spike neurons; *Off,* REM-on, PGO-off neurons; *Post,* post-PGO neurons. Abbreviations other than PB and LDT: *AQ,* aqueduct; *BP,* brachium pontis; *CG,* central gray; *FTC,* central tegmental field; *IP,* interpeduncular nucleus.

charge pattern of their PPIHs (see Materials and Methods). The selection of these 80 cells was imposed by the minimum number of PGO events and related PB/LDT discharges required for quantitative analyses (see Materials and Methods). PPIHs could detect the presence of short (3–10 msec) and very short (<3 msec) intervals reflecting slow- and high-frequency spike bursts or the presence of medium-class intervals (10–30 msec) betraying tonic repetitive single spikes. The neuronal population used for single-cell or pooled-cell analyses of time course and discharge patterns of peri-PGO activity comprised 53 PB and 27 LDT neurons. The location of different types of PGO-on and PGO-off cells is shown in Figure 1. Since the same PGO-related cellular types were observed in PB and LDT nuclei, we use the global term PB/LDT unless we refer to a particular cell or neuronal group.

Of those 80 analyzed neurons, 32 were antidromically identified (Fig. 2*A,B*) from different thalamic nuclei: LG (n = 11); pulvinar-lateroposterior complex (n = 11); rostral intralaminar centrolateral-paracentral complex (n = 8); and anterior complex (n = 2). In some instances, the antidromic invasion was followed by a synaptically evoked high-frequency spike burst (Fig. 2*C*). The identified thalamic-projecting cells belonged to all 6 cell types described below, including the PGO-off neurons. No differences were found between thalamic-projecting cells and neurons that remained unidentified by antidromic testing as far as the time course or discharge patterns of their PGO-related activity were concerned.

PGO-on sluggish-burst neurons

This cell class (n = 30; 16% of PGO-related neurons) is the only one that was described in earlier studies (see introductory remarks). Typically, the PGO-related activity of these cells consisted of a stereotyped burst of 2–5 spikes with an intraburst frequency of 120–180 Hz, preceding the negative peak of LG-PGO waves by 20–40 msec (Fig. 3). Occasionally, the PGO-related activity consisted of a single spike (see panels 2, 4, and 5 in Fig. 3). The stereotyped characteristics of these bursts suggest that they reflect LTSs (see Discussion). It is therefore not surprising that single action potentials arose from tiny LTSs. The oscilloscopic traces (Fig. 3) and especially the PPIH analysis (Figs. 4*A,B*; 13*A*) revealed the low frequency of these PGO-on bursts. Because an intraburst frequency of 120–180 Hz is well below the usual frequency (>250 Hz) of a burst triggered by LTS-generating thalamic neurons, we use the term "sluggish" to define such bursts.

Another defining characteristic of PGO-on sluggish-burst neurons was the low rate of their spontaneous firing throughout the waking–sleep cycle (<4 Hz, or even <2 Hz). This contrasted with the high firing rate of a second class of bursting cells, described below. Moreover, the firing rate of some sluggish-burst neurons diminished from W and S to REM sleep, which is quite an exceptional feature of PB/LDT neurons (Fig. 4*C*). These elements were probably not monoaminergic because they were not silent during REM sleep and discharged selectively in relation with PGO waves. In neurons with spontaneous firing rates inferior to 1 Hz during REM sleep, the PGO-related discharges represented more than 70% of the total number of spikes throughout REM sleep, whereas in neurons with higher firing rates (3–4 Hz), the percentage of PGO-related discharges was 10% or less (see the 2 cells in Fig. 4*A,B*).

PGO-on neurons with high-frequency bursts and tonic discharges

We now describe a class of PGO-on cells in PB and LDT nuclei that discharged high-frequency spike bursts on a background of tonically increased firing rate during REM sleep (n = 42; 22% of PGO-related neurons). This neuronal type is therefore distinct from the group of PGO-on sluggish-burst neurons, described above, by at least 3 characteristics: (1) the much higher intraburst frequency (>500 Hz); (2) the much higher rate of background firing during REM sleep (10–40 Hz); and (3) the fact that PGO-on bursts were triggered after a period of progressive acceleration of spontaneous discharges, preceding the PGO-on burst by about 150–200 msec (see oscilloscopic traces in Fig.

5). Furthermore, by contrast with the PGO-on sluggish-burst neurons, these cells had spontaneous firing rates higher than 10 Hz during both W (mean, 18 Hz) and EEG-synchronized sleep (mean, 11 Hz).

The analysis of discharge patterns in such a neuron is documented in Figure 6. It essentially shows that (1) the bursts preceded by 30–50 msec the negative peak of the LG-PGO wave, that is, a lead time similar to that seen in PGO-on sluggish-burst cells; (2) when separate analyses were made for clustered PGO waves, the PPSHs showed rhythmic peaks of increased discharges with periods around 120 msec, reflecting the recurrence of PGO waves within a cluster (Fig. 6*A*); (3) the majority of PGO-related interspike intervals were distributed between 1 and 2.5 msec, reflecting maximum intraburst frequencies exceeding 500 Hz (see PPIHs in Fig. 6*A*); (4) because of their high level of spontaneous discharges throughout REM sleep, the proportion of interspike intervals related to single PGO waves was less than 5–10% of the total number of intervals during REM sleep; and (5) the ISIHs indicated high rates and tonic discharges during W and S (Fig. 6*B*), as well as a tonic increase in discharge frequencies during REM sleep, with the PGO-on bursts superimposed as a mode at 2–3 msec (Figs. 6*B*). The latter aspect emphasizes that a certain class of neurons discharging tonically during all states of vigilance can also be effective in the phasic process of triggering PGO-on bursts. Some of these neurons (e.g., the cell depicted in Fig. 6) also displayed signs of precursor increased activity prior to EEG desynchronization in REM sleep (see Steriade et al., 1990).

PGO-on tonic neurons

A group of 38 PB/LDT neurons (20% of PGO-related cells) discharged tonic repetitive single spikes preceding the LG-PGO waves. Some of them discharged at rather low rates (<8 Hz) during REM sleep and their PGO-on trains of single spikes at 25–40 Hz were easily distinguishable (top cell in Fig. 7). The majority, however, had higher spontaneous firing rates (10–20 Hz) during REM sleep and reached frequencies of 70–80 Hz within their PGO-on spike trains (bottom cell in Fig. 7). However, these cells never discharged high-frequency spike bursts spontaneously or in relation with PGO waves.

The PPSHs and PPIHs in this cell group revealed an increased activity preceding the LG-PGO wave by 80–150 msec, and a distribution of PGO-related interspike intervals between 10 and 30 msec (Fig. 8*A*). The ISIHs showed tonic discharge patterns during all states of vigilance, with quite symmetrical shapes, relatively small dispersion around the modes (at 50–70 msec), and virtual absence of short (<10 msec) intervals in W and S, whereas the shorter interval modes (10–30 msec) during REM sleep reflected the PGO-on tonic spike trains (Fig. 8*B*). In terms of discharge rates, this cell class belongs to the vast majority of fast- and tonically-discharging PB/LDT neurons (see companion paper).

PGO-on single spikes

Eighteen PB or LDT cells (10% of PGO-related neurons) discharged single spikes, doublets, or triplets that preceded by 15–30 msec the LG-PGO waves (Figs. 9, 10).

There are 2 differences between this cellular class and the PGO-on tonic neurons, as well as PGO-on sluggish-burst neurons. First, whereas the spike trains of PGO-on tonic cells had at least 5 but most often 7 up to 20 action potentials, PGO-on single-spike neurons usually discharged a single action potential prior to isolated PGO waves or to the first wave in a PGO cluster (Fig. 9, panels 1, 2, and 4). This feature was reflected in the PPIHs of such neurons that lacked the medium-class intervals (10–30 msec) which constituted the PGO-related activity of tonic cells. Second, the PGO-related discharge of these neurons occurred less than 50 msec before the PGO wave (compared with 80–150 msec for PGO-on tonic cells). The doublets and triplets of PGO-on single-spike cells were separated by interspike intervals of 15–20 msec. They are, therefore, basically different from the PGO-on cells with sluggish-burst, in which the majority of interspike intervals were between 5 and 10 msec.

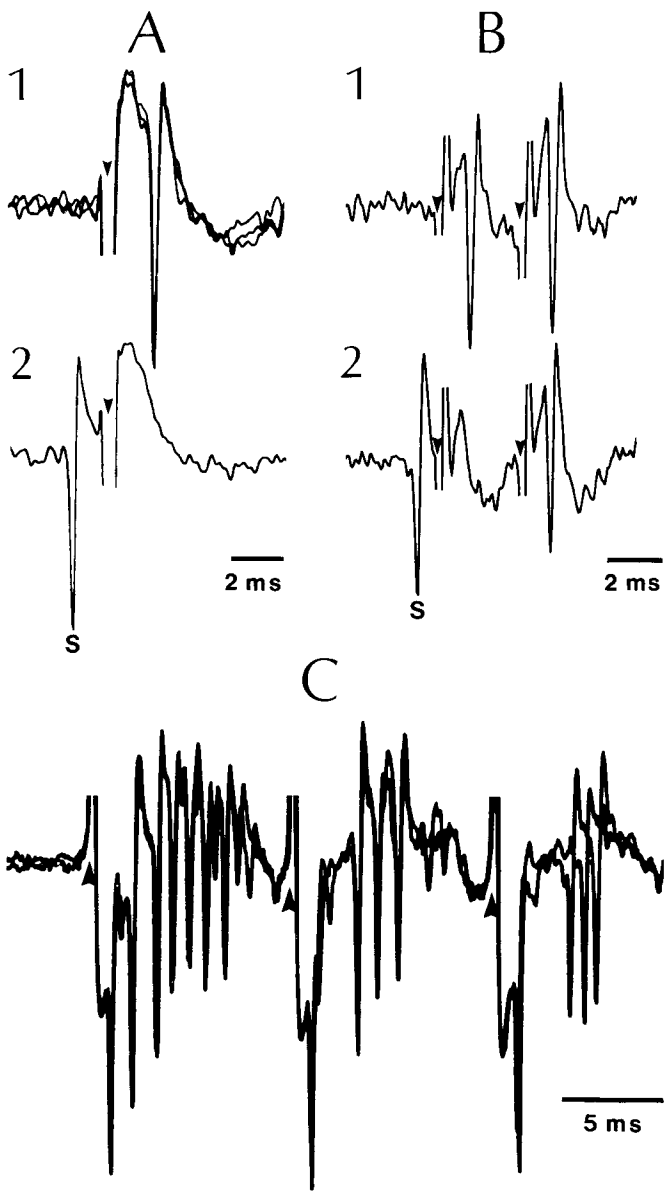

Figure 2. Antidromic identification of thalamic projections of PGO-related neurons. Stimuli marked by arrowheads. *A*, Sluggish-burst neuron projecting to the medial thalamus. In *2*, collision with a spontaneous (*S*) discharge. *B*, PGO-on high-frequency burst cell (same neuron as in Figs. 5, 6) backfired from the lateral geniculate nucleus. In *2*, collision of the first antidromic response with a spontaneous (*S*) spike. *C*, PGO-on high-frequency burst neuron with antidromic spike evoked from the lateral geniculate nucleus, followed by synaptic spike burst. Note progressive decrease in spikes within bursts evoked by 2nd and 3rd stimuli.

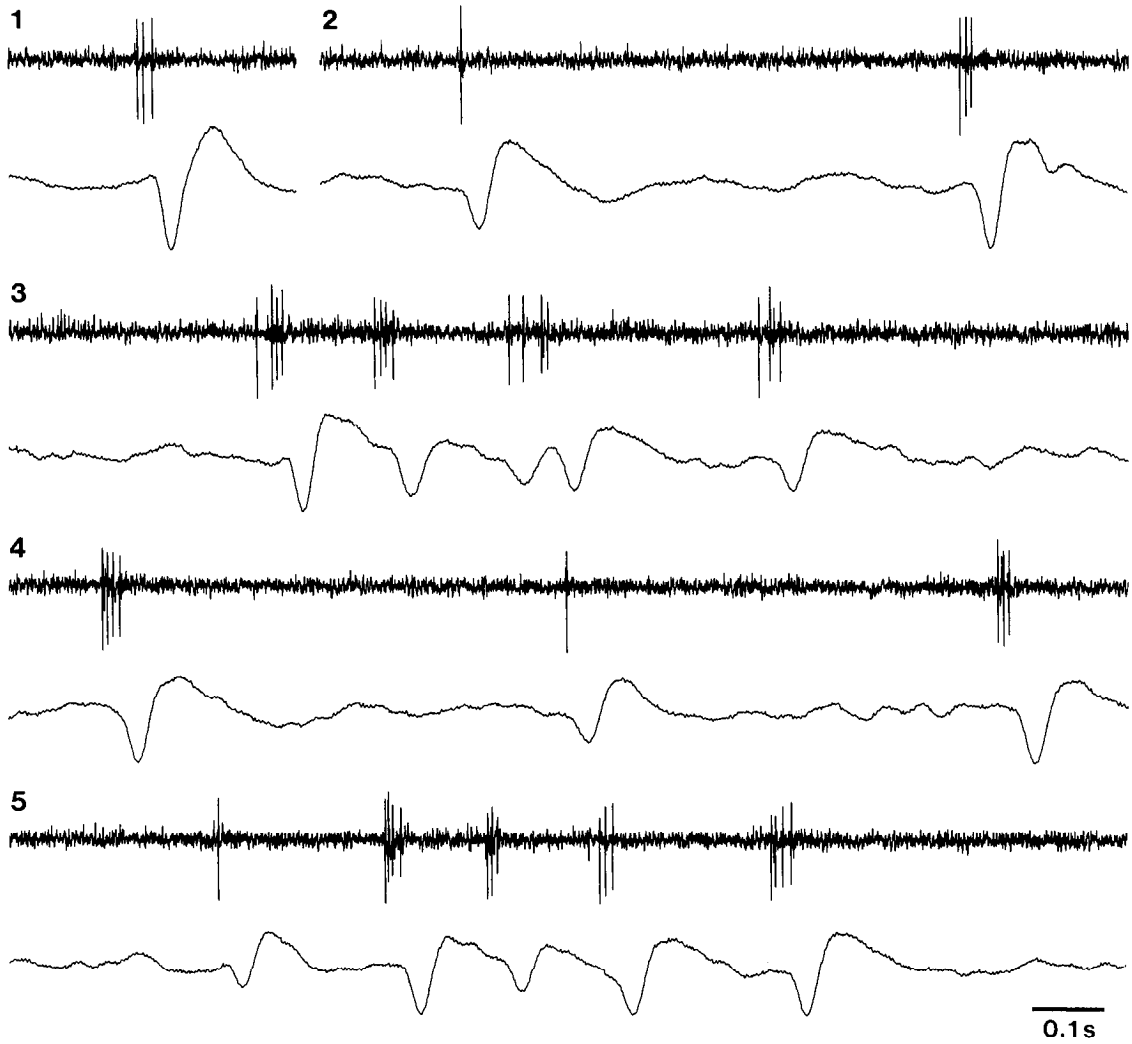

Figure 3. PGO-on sluggish-burst cell. The 2 traces depict the activity of a PB neuron (antidromically identified from the LG thalamic nucleus) and the LG-PGO field potential.

PGO-on single action potential probably arises from conventional excitatory postsynaptic potentials (EPSPs) and not from tiny LTSs (see Discussion).

PGO-off neurons

PGO-off neurons (n = 16; 8% of PGO-related cells) probably represent the most unexpected cell type in PB/LDT cholinergic nuclei (Figs. 11, 12). Out of 16 neurons, 2 were antidromically identified from anterior and rostral intralaminar thalamic nuclei. All these neurons discharged tonically, in a clocklike manner, with firing rates exceeding those of all other PB/LDT neuronal types (20–25 Hz in W and S), and they further increased their discharge frequencies passing to REM sleep (above 30 Hz). The fact that such neurons ceased firing 50–180 msec before the LG-PGO wave, but occasionally as long as 300 msec prior to the PGO wave (see Fig. 12*B*), led us to term them REM-on, PGO-off cells. The cessation of firing lasted over the whole negative deflection of the thalamic PGO field potential, but in some instances the diminution in firing rate lasted for 100–200 msec after the full development of the negative–positive LG-PGO wave.

Post-PGO neurons

This neuronal class (n = 43; 23% of PGO-related cells) fired spike bursts related to the ascending limb of the negativity and the subsequent slow positivity of LG-PGO waves (60–80 msec after T_0 of PGO wave) or fired tonically for much longer periods of time, up to 300 msec after T_0 of PGO waves (see Fig. 13*E*). These neurons also belonged to the class of fast and tonically discharging neurons described in the companion paper.

Pooled analyses in different PGO-related cellular types

Figure 13 depicts the PPSHs and PPIHs of 40 PB/LDT neurons belonging to 5 cellular classes described above: sluggish-burst neurons (*A*), high-frequency bursts occurring on a background of increased neuronal firing (*B*), PGO-on tonic cells (*C*), PGO-off cells (*D*), and post-PGO neurons (*E*). PGO-on neurons discharging single spikes were not included because we could not determine with extracellular recordings whether single spikes arose from EPSPs or from tiny LTSs (but see the results of parallel experiments with intracellular recordings in the Discussion). The assembly in Figure 13 provides a synoptic view

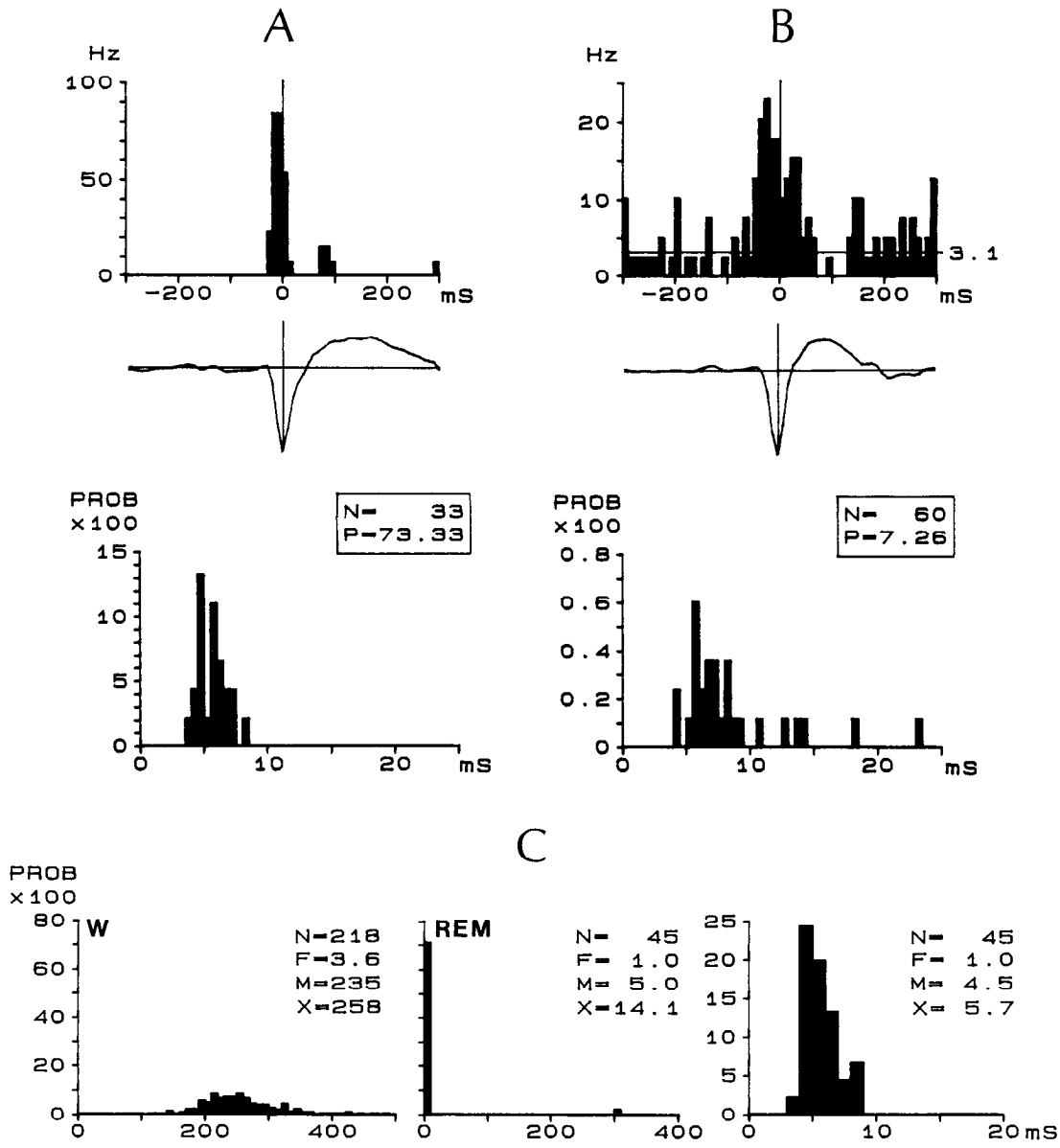

Figure 4. Analyses of PGO-related discharges in 2 PB neurons. In both *A* and *B*, the *upper row* depicts PPSHs (10 msec bins), the *middle row* depicts averaged PGO waves from the analyzed epoch, and the *lower row* depicts PPIHs (1 msec bins). Symbols in PPIHs: *N*, number of intervals within the bins with PGO-on activity; *P*, percentage of intervals within the PGO-on epoch out of the total number of intervals during the analyzed epoch of REM sleep. In this and following similar figures, the level of background discharges (spikes/sec) preceding the PGO-related activity is also indicated on PPSHs (0 Hz in *A*, 3.1 Hz in *B*). *C*, ISIHs, during W and REM sleep, of cell depicted in *A*. Two types of ISIHs are shown: with 10 msec bins (*W* and *left* REM sleep) and 1 msec bins (*right* REM sleep). Symbols in ISIHs: *N*, number of intervals; *F*, discharge frequency (spikes/sec); *M*, interval mode; *X*, mean interval (in the depicted time range).

of the striking variety of PGO-related neurons disclosed in PB/LDT nuclei.

The salient findings in these pooled analyses can be summarized as follows. (1) Sluggish-burst cells have the lowest level of background firing during REM sleep (1.1 Hz) and most intervals of their PGO-on activity are distributed between 5 and 10 msec. (2) High-frequency bursts (most intraburst intervals <3 msec) lead the PGO waves by about 30 msec and are preceded by an acceleration of spontaneous discharges whose onset is about 150 msec before the PGO-on burst (see also the oscilloscopic traces in Fig. 5). (3) The longest-lead PGO-on neurons in PB/LDT nuclei (150 msec before the thalamic PGO wave) are tonically discharging elements, with most intervals between 10 and 30 msec. (4) The rates of background firing in PGO-off tonic cells are near 40 Hz in REM sleep, and their PGO-related activity is the reciprocal image of the PPSH depicting PGO-tonic cells. (5) Post-PGO neurons discharge for 300 msec after the PGO waves and their discharges are tonic (most intervals between 10 and 30 msec, similar to PGO-on tonic neurons). We speculate about the possible synaptic relations and transmitter actions in these neuronal types in the discussion.

Phasically discharging PB/LDT neurons in relation to orienting reactions during W and REM sleep

Because EMPs and PGO waves are viewed as correlates of orienting reactions during W and REM sleep (see Discussion), we

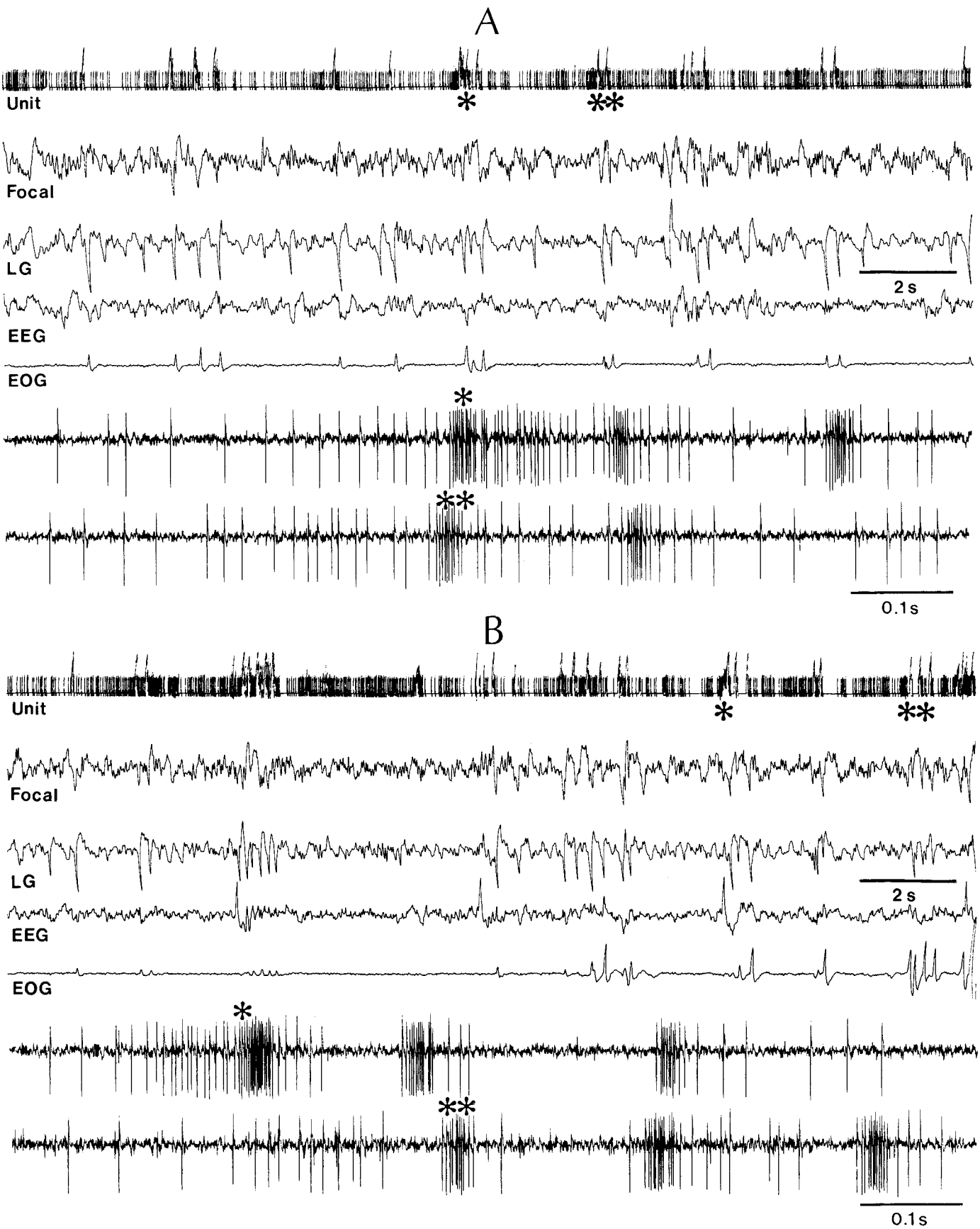

Figure 5. Activity of a PGO-on high-frequency burst cell, recorded from the PB area and antidromically activated from the thalamic LG nucleus (see identification of this neuron in Fig. 2*B*). *A* and *B*, Two different epochs during REM sleep. In each of these epochs, 5 ink-written traces and 2 oscilloscopic traces are illustrated. Ink-written traces depict (from *top* to *bottom*) action potentials of PB unit (deflections exceeding the common level of single spikes represent high-frequency bursts), focal waves recorded simultaneously by the same microelectrode in PB area, LG field

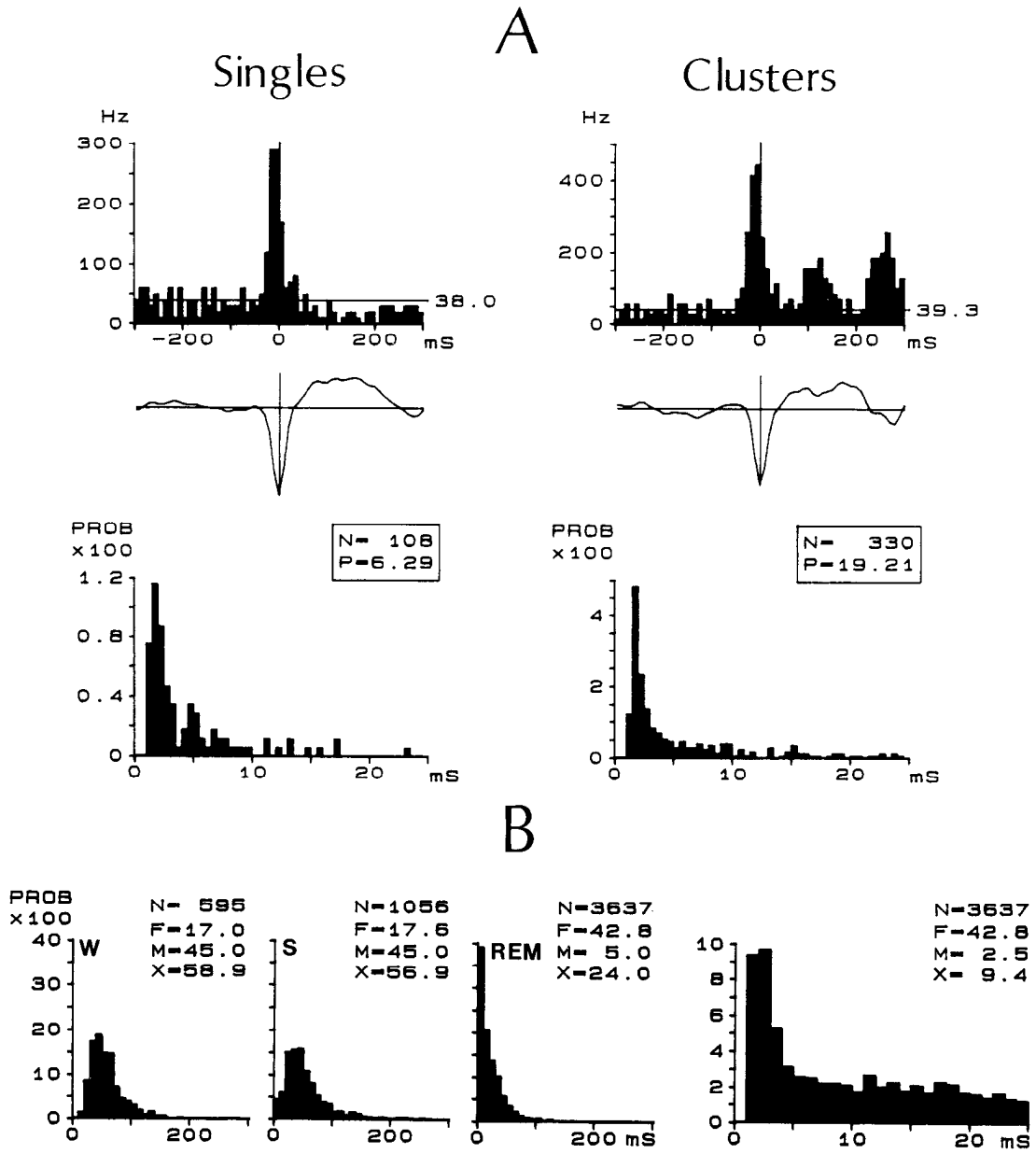

Figure 6. PPSHs and PPIHs of single and clustered PGO waves for the cell depicted in Figure 5. Same graphic arrangement and symbols as in Figure 4*A, B*. In *B*, ISIHs (10-msec bins) of the same cell during W, S, and REM sleep. Right ISIH is also from REM sleep, but with 1-msec bins). For symbols in ISIHs, see Fig. 4*C*.

have compared the PGO-related discharges of 14 PB cells to their responses evoked by auditory (hand-clapping) stimuli during W and REM sleep. Four of these neurons were identified antidromically from various thalamic sites.

During W, auditory stimuli evoked high-frequency (400–600 Hz) spike bursts in an otherwise tonically discharging PB cell (Fig. 14). The bursts were associated with negative–positive field potentials recorded simultaneously by the same microelectrode in the PB area. These responses habituated by increasing the stimulus rate, as seen from the lower amplitude of PB field potentials and the progressive diminution in the number of action potentials within the evoked bursts (Fig. 14). The related field potentials recorded from the thalamic LG nucleus were initially positive (that is, of opposite polarity compared to the negative–positive LG-PGO waves during REM sleep), probably because the auditory stimulus evoked a negative field potential

←

potentials, EEG waves from the anterior suprasylvian gyrus, and eye movements. Note high-frequency bursts closely related to PB-PGO and LG-PGO waves. In *A*, groups of 3 high-frequency bursts (*1 asterisk* on ink-written trace) and 2 high-frequency bursts (*2 asterisks*) are depicted below with original spikes. In *B*, groups of 3 high-frequency bursts (*1 asterisk* on ink-written trace) and again 3 high-frequency bursts (*2 asterisks*) are also depicted below with original spikes. Note in oscilloscopic traces: progressive acceleration of discharges preceding the burst by about 100–150 msec.

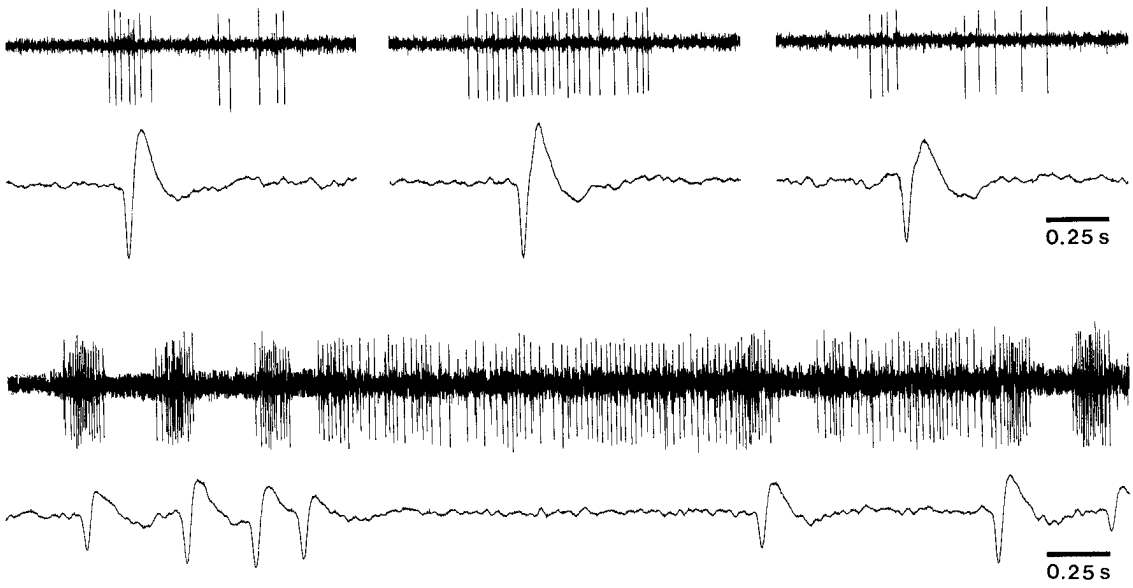

Figure 7. PGO-on tonic cells recorded in LDT (*top*; antidromically activated from lateroposterior thalamic nucleus) and PB (*bottom*). In both neurons, unit activities are displayed simultaneously with LG-PGO waves.

with maximum amplitude in the medial geniculate nucleus and we recorded a reversed wave in the overlying LG nucleus. These differences between LG-PGO waves during REM sleep and auditory-evoked field potentials during W is depicted in Figures 14–16.

A similar activity pattern during W is depicted for another PB cell that did not show a PGO-related activity during REM sleep (Fig. 15*A*). In W, the initial high-frequency core of the sensory-evoked spike burst was followed by a tonic tail (see bursts 1–2 in Fig. 15*B*). Note that habituation of the auditory-evoked responses, occurring with increasing frequency of stimuli, appeared as a diminution of field potentials in the PB area, whereas thalamic EMPs and eye movements completely ceased when stimulus frequency was increased from 1/sec to 2/sec (Fig. 15*B*).

Auditory stimuli evoked PB field potentials and PB-cell's spike bursts during REM sleep as well, with signs of habituation by stimulus repetition, but these brain-stem responses were not reflected in the thalamus (Fig. 16*A*). In some REM sleep epochs, the same neuron discharged spike bursts related to spontaneous PGO waves in the PB area (Fig. 16*B*). During W, this neuron displayed auditory-evoked field and unit responses that were similar to those of the other PB cells (Fig. 16*C*).

Discussion

We have shown that neurons in the mesopontine cholinergic nuclei involved in the transfer of PGO waves to the thalamus do not constitute a homogenous cell class. Rather, numerous neuronal types take part in this process. In the experimental conditions of a behaving preparation, it is impossible to determine with extracellular recordings whether the various cell groups described here correspond to distinct anatomical classes using the same or different neurotransmitter(s). The distinctness of neuronal categories is based on their firing patterns and time relation with thalamic PGO waves. Some of these cell groups appeared to possess electroresponsive properties similar to those that have recently been described in various classes of PB/LDT neurons studied *in vitro* (see below). We now discuss the discharge patterns of PGO-related neurons, their place in various brain-stem circuits, and their possible involvement in PGO genesis.

PGO-on burst neurons

Our data disclosed the existence of 2 distinct types of PGO-on burst cells in both PB and LDT nuclei, each of them having projections to thalamic nuclei.

1. The sluggish-burst neurons resemble the only cellular type of PGO-on cells described in earlier studies. These bursts were viewed until now as resulting from disinhibition of cholineregic neurons, subsequent to the cessation of firing in presumed inhibitory monoaminergic cells during REM sleep (see introductory remarks).

We postulate that such bursts are triggered by LTSs deinactivated by membrane hyperpolarization. Our proposal is based on 2 observations: the stereotyped features of these bursts and their occurrence on a background of very low discharge rate of PB/LDT neurons (<2 Hz). Indeed, the firing rate of some sluggish-burst cells diminished significantly from W to REM sleep (see Fig. 4*C*), an exceptional finding for PB/LDT cells (Steriade et al., 1990). Of course, the intraburst frequency (120–180 Hz) of these cells is rather low compared with the bursts triggered by LTSs in other cellular types (see Steriade and Llinás, 1988). However, this difference does not necessarily invalidate our hypothesis since it could be attributed to a variety of factors, such as the remote location of the underlying T-channels (Coulter et al., 1989). In fact, Kang and Kitai (1990) have reported that the duration of LTSs of rat's pedunculopontine neurons is much longer (50–150 msec) than that described in thalamic neurons; besides, the intraburst frequency of action potentials which crown the LTS appears to be lower than 200 Hz (see their Fig. 1, *A, D*).

That some PB/LDT neurons indeed possess a calcium conductance underlying LTSs has been demonstrated *in vitro* in

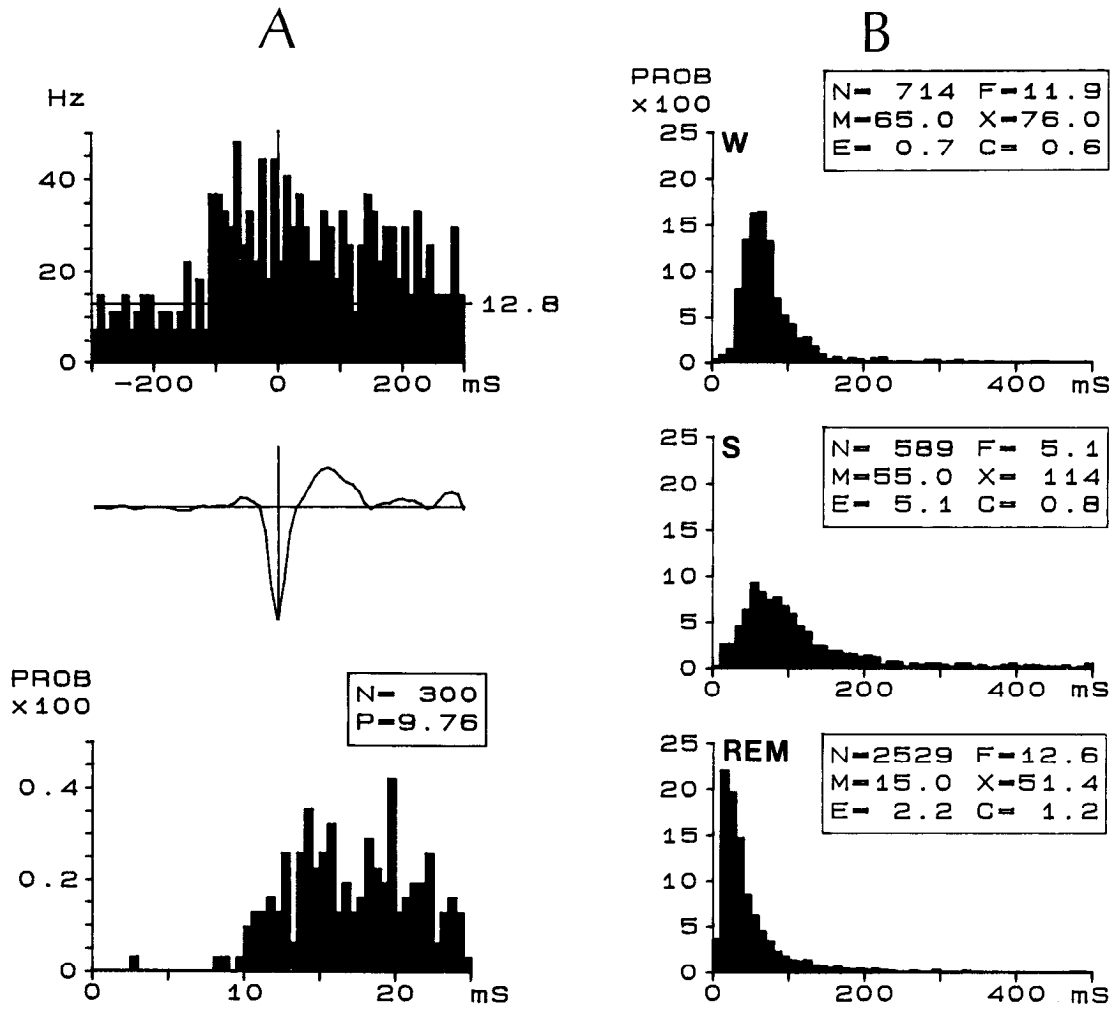

Figure 8. Activity patterns of a PGO-on tonic PB cell projecting to the LG thalamic nucleus. *A*, PPSH, averaged PGO waves, and PPIH. *B*, ISIHs (10-msec bins) of the same neuron across the waking–sleep cycle. For symbols in PPIH and ISIHs, see preceding figures. Additional symbols in ISIHs: *E*, proportion of intervals in excess of the depicted time range; *C*, coefficient of variation.

guinea pig (Leonard and Llinás, 1987, 1990; Wilcox et al., 1989) and rat (Kang and Kitai, 1990). In both species, these cells represent a minority of mesopontine neurons and have been shown to be *noncholinergic* with the cholinergic marker NADPH-diaphorase (Leonard and Llinás, 1987, 1990; Wilcox et al., 1989) and ChAT immunohistochemistry (Kang and Kitai, 1990). In the study by Leonard and Llinás (1990), LTS neurons were not identified as projecting to the thalamus (slices were prepared several days after retrograde tracer injections in the thalamus). Yet, we are not the first to report that low-frequency bursting PGO-on neurons can be activated antidromically from the thalamus in the cat (see Sakai, 1985). Whether this reflects a species difference between cat and guinea pig remains unclear.

At first sight, the noncholinergic nature of LTS cells may seem puzzling. Indeed, until now, this was the only cell class considered as the executive factor in the transfer of PGO waves to the thalamus, and consistent evidence shows that thalamic PGO waves are the result of a nicotinic-mediated event (Ruch-Monachon et al., 1976; Hu et al., 1988). If the noncholinergic nature of LTS neurons in PB/LDT nuclei should be definitely established in cat, we may admit that these cells contribute an additional brain-stem contingent to that of PGO-on cholinergic cells (see below). In all likelihood the PGO-on sluggish-burst elements are *not* monoaminergic, as they discharged selectively in association with PGO waves, whereas all available evidence indicates that monoamine-containing cells in locus coeruleus, dorsal raphe, or outside these nuclei are virtually silent during REM sleep (see Steriade and McCarley, 1990).

Assuming that LTSs underlie the PGO-on sluggish-bursts, which are the possible sources in brain-stem circuits that would create a hyperpolarization upon which excitatory impulses of central origin would trigger LTSs or would induce phasic hyperpolarizations of sufficient magnitude to trigger rebound LTSs? Two major possibilities are open.

First, there is the GABAergic input from substantia nigra pars reticulata (SNr) neurons to the pedunculopontine nucleus. This pathway (Beckstead, 1982; Beckstead and Frankfurter, 1982) was stimulated and the effects upon pedunculopontine neurons were found to be mainly inhibitory, both *in vivo* (Scarnati et al., 1987) and *in vitro* (Kang and Kitai, 1990). In parallel experiments, we have recorded SNr cells across the wake–sleep cycle, and 35% of such cells displayed an increased activity 50–150 msec prior to the thalamic PGO wave (Datta et al., 1990).

Second, the cholinergic neurons of the PB/LDT nuclei them-

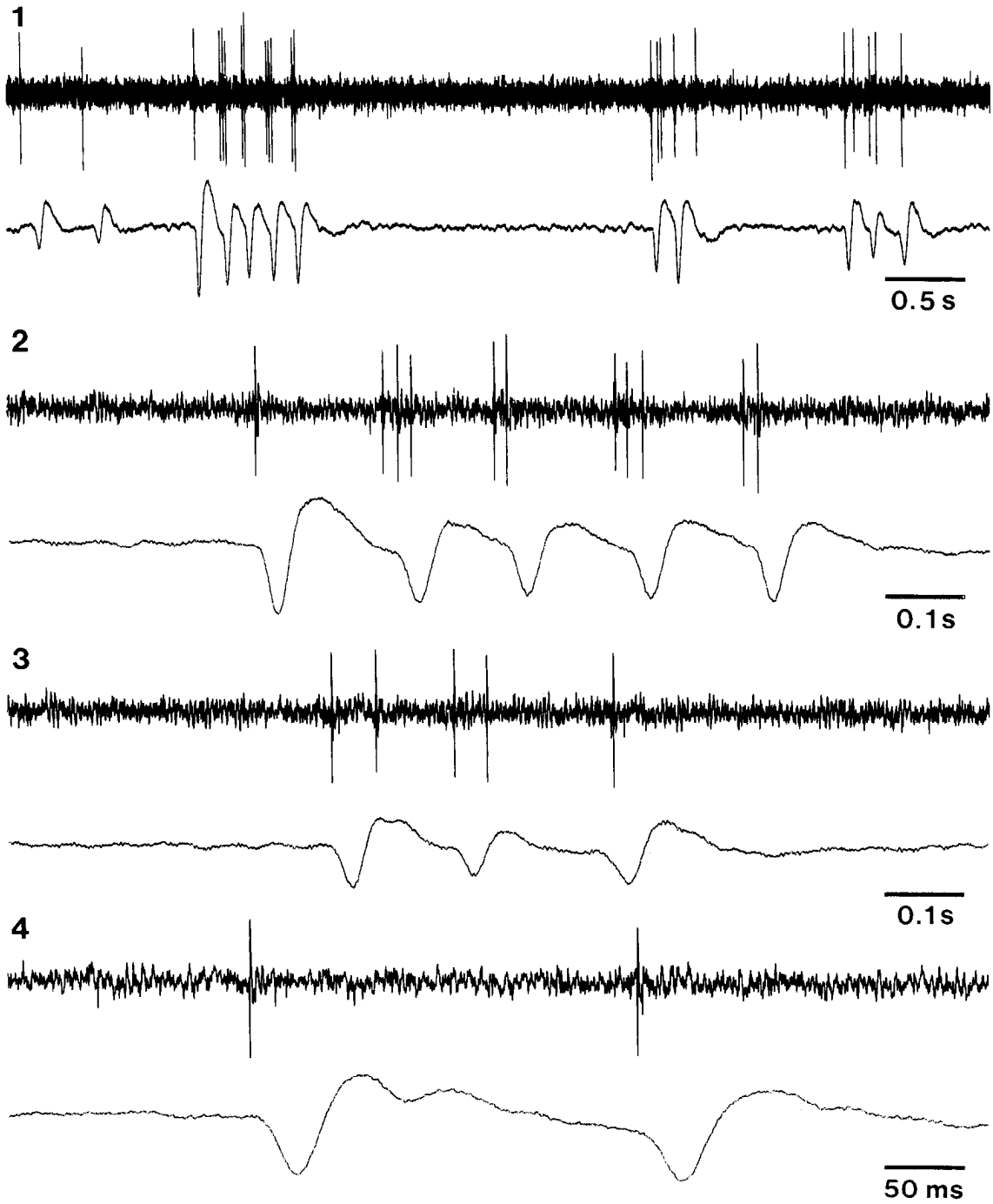

Figure 9. PGO-on LDT neuron discharging single spikes, doublets or triplets. See also text.

selves may be the source of the hyperpolarization. PGO-on tonic neurons, presumably cholinergic (see below), may inhibit adjacent neurons in the PB/LDT nuclei through local axonal collaterals, thus providing the necessary background of hyperpolarization to deinactivate the LTSs. This proposal is based on *in vitro* experiments showing that ACh induces hyperpolarizing effects (by activating a potassium conductance via muscarinic receptors of the M2 class) upon parabrachial cells (Egan and North, 1986; Christie and North, 1988) and pedunculopontine and LDT neurons, some of them possessing the LTS conductance (Leonard and Llinas, 1988).

2. The PGO-on neurons with high-frequency bursts (Figs. 5, 6, and 13*B*) are one of the most intriguing neuronal classes disclosed in this study because their bursts, distinct from the sluggish type, occur upon a background of tonically increased firing during REM sleep. It suggests that, instead of being deinactivated by hyperpolarization, these may be high-threshold bursts triggered at a relatively depolarized level. The fact that the bursts were preceded by a progressive acceleration of spontaneous discharges is consistent with this view (see an alternative possibility in the section on PGO-on tonic neurons). Although high-threshold bursts have not been detected in studies of PB/

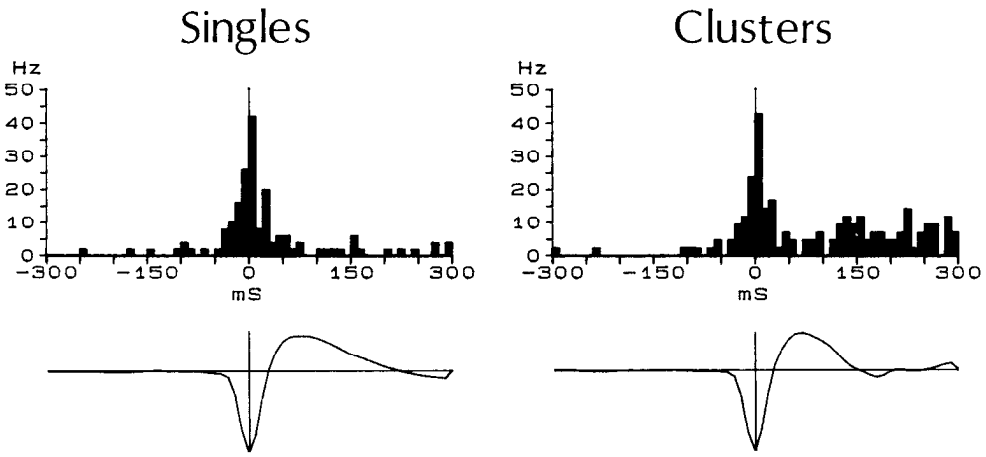

Figure 10. PPSHs (*top*) and averaged singles and clustered PGO waves (*bottom*) for the neuron depicted in Figure 9.

LDT neurons *in vitro,* they were observed in 9% of medial pontine reticular neurons *in vitro* (see Fig. 1C in Gerber et al., 1989). In those medial pontine cells, the threshold of the fast action potential had to be crossed prior to activation of the burst. This particular electroresponsiveness may be taken as evidence for a high-threshold calcium conductance, possibly located in the distal dendrites.

Given that these neurons discharged at high rates and that some increased their rate of discharges tonically prior to REM sleep, bursting and tonic discharge features may coexist in the same neuron.

PGO-on tonic neurons

These cells exhibited the longest lead time (150 msec) with respect to thalamic PGO waves among all PGO-on cells. The absence of bursts in this neuronal type was ascertained by a negligible proportion of very short intervals in PPIHs and ISIHs across the waking–sleep cycle (Figs. 8, 13*C*). This fact emphasizes the distinction between PGO-on neurons displaying high-frequency bursts and purely tonic cells.

The discharge pattern of PGO-on tonic neurons suggests that they correspond to a cellular class described in PB/LDT neurons studied *in vitro,* firing repetitively upon depolarizing current pulses, displaying a delay in the return to baseline potential following a hyperpolarizing pulse (by activating a transient outward, A current), lacking the LTS conductance, and being identified as thalamic-projecting as well as cholinergic (Leonard and Llinás, 1988, 1990; Kang and Kitai, 1990). Thus, these neurons are representative of PB/LDT cells qualifying for tonic cells across the waking–sleep cycle. We showed in the present study that tonic cells—which are among the best candidates for the maintenance and probably also the induction of enduring EEG desynchronization (Steriade et al., 1990)—are also involved in the transfer of phasic PGO events to the thalamus. Again, this defies the simplistic assumption that neurons should be classified according to their participation in tonic and phasic processes.

There exists corroborative evidence to help explain the high rates of background firing in PGO-on tonic, presumably cholinergic cells. The tonic cholinergic cells studied *in vitro* are larger than LTS neurons (Kang and Kitai, 1990; Leonard and Llinás, 1990). Cholinergic cells in the pedunculopontine nucleus are larger than other cellular types in that region or in the more caudal parabrachial complex (see Wainer and Mesulam, 1990). Furthermore, an ultrastructural study of the pedunculopontine nucleus in the cat revealed that the bouton coverage ratios in large cells is more than 3 times higher than those in small cells, suggesting that cholinergic cells receive more synaptic inputs with respect to their somatic surfaces (Moriizumi et al., 1989). In this context, it is possible to assume that the difference between PGO-on tonic and single-spike discharging neurons is quantitative rather than qualitative, reflecting different degrees of synaptic drive.

Could tonic cells activate some neurons within the PB/LDT nuclei? This question arises from the observation that tonic cells begin to increase their activity about 150 msec before the thalamic PGO wave. This increase in discharge rate coincides with the progressive acceleration of discharges occurring in high-frequency bursting cells before the thalamic PGO wave (see Fig. 13, *B, C*). If the A-current is inactivated at depolarized levels, as is probably the case with PB/LDT cells firing at high rates during REM sleep, the 100–120 msec excitation exerted by PGO-on tonic cells upon PGO-on high-frequency burst cells would not be attenuated and might eventually give rise to a high-frequency burst. However, the idea that tonic, presumably cholinergic, cells create a background of increased firing in neurons that ultimately discharge PGO-on high-frequency bursts is not compatible with data indicating a muscarinic-mediated hyperpolarization of tonic PB/LDT neurons (Leonard and Llinás, 1988). The possibility remains that a nicotinic excitation has not yet been detected, possibly because of the rapid desensitization of nicotinic receptors.

PGO-on neurons discharging single spikes

Because extracellular recordings do not allow the study of mechanisms underlying the genesis of single spikes (conventional EPSPs or small-size and slowly developing LTSs?), we conducted parallel intracellular experiments on brain-stem events leading to thalamic PGO waves in reserpine-treated cats (Paré et al., 1990). Similarly to data reported in the present study (see Figs. 9, 10), some PB cells fired single spikes or spike doublets preceding the LG-PGO wave by 10–30 msec. Upon impalement, it became clear that the PGO-on action potential was triggered by an EPSP which increased in amplitude with membrane hyperpolarization and was usually crowned by fast-rising wavelets. Those neurons lacked LTSs even when large hyperpolarizing pulses were applied.

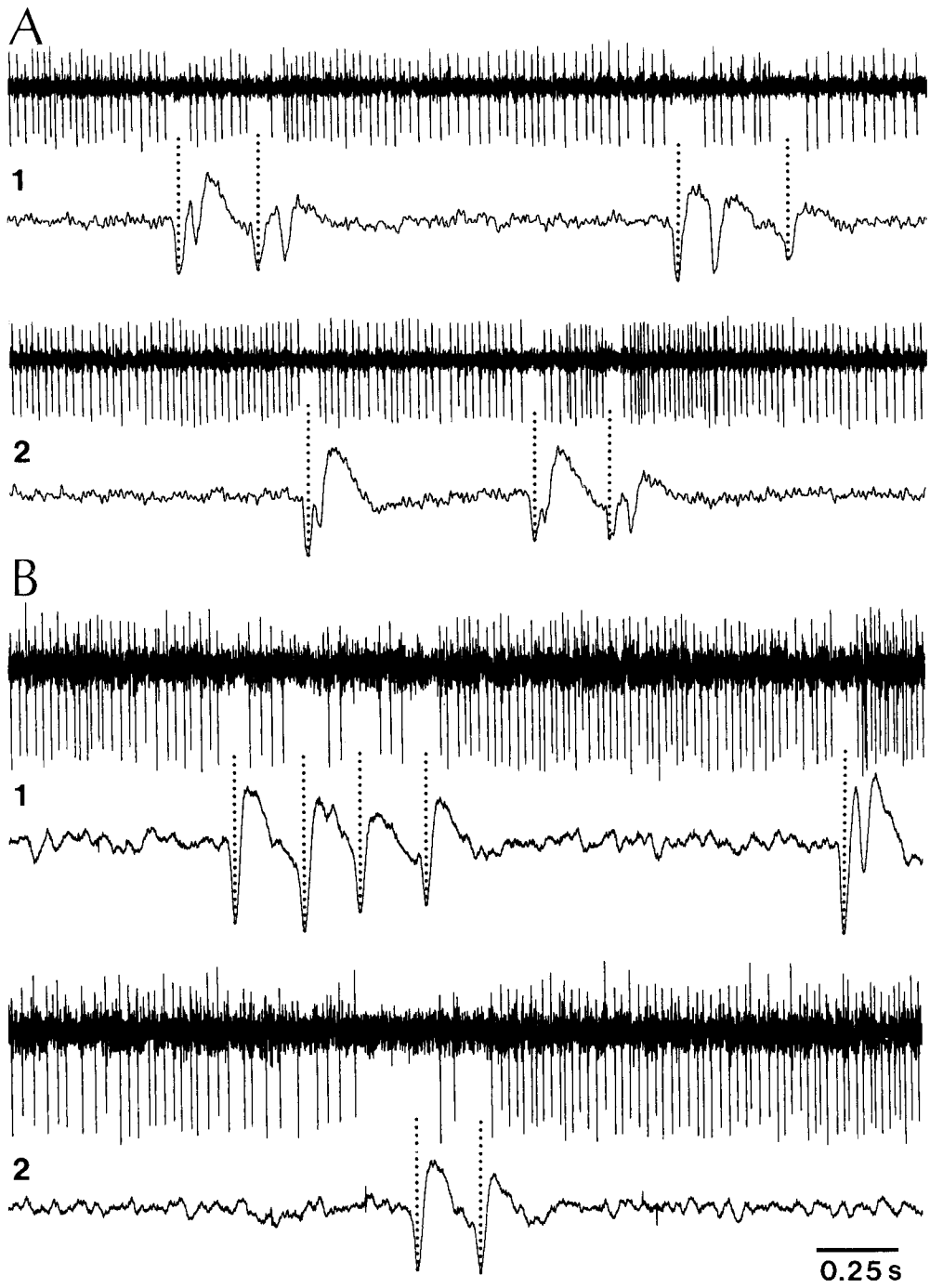

Figure 11. REM-on, PGO-off neurons. Both neurons (*A* and *B*) recorded from LDT nucleus (neuron *B* antidromically activated from the anterior thalamic complex). Two traces as in Figure 3 and other similar figures. *Dotted lines* indicate the peak negativity of the LG-PGO waves. Note cessation of firing during fully developed PGO waves (*left* parts of *B1, 2*), as well as during the first, but not the smaller second, wave of a biphid PGO complex (*A1, 2* and *right* part in *B1*).

PGO-off neurons

We hypothesize that this REM-on, PGO-off neuronal class is GABAergic for the following reasons. (1) The firing rates of PGO-off neurons were significantly higher during all states of vigilance than in any other neuronal type recorded in brainstem cholinergic and noncholinergic nuclei. In other structures, GABAergic neurons also discharge at high rates. Such is the case for cerebellar Purkinje cells (Eccles et al., 1967), SNr neurons (Deniau et al., 1979; Hikosaka and Wurtz, 1983; Datta et al., 1990), and reticular thalamic neurons (Steriade et al., 1986). It is known that the calcium-binding protein parvalbumin is found in GABAergic neurons. This was shown for identified GABAergic elements and for parvalbumin-immunoreactive cells whose distribution overlapped with that of GABAergic neurons (Celio and Heizmann, 1981; Jourdain et al., 1989). Celio (1986) has suggested that this calcium-binding protein would prevent the activation of the calcium-dependent potassium current, thus reducing the afterhyperpolarizing potentials and spike accommodation, with the consequence of increasing the discharge frequency of the neuron. (2) A population of LDT cells is immunoreactive to GABA-synthesizing enzyme, and no pontine perikarya have been found to contain immunoreactivity for both GAD and tyrosine hydroxylase (Kosaka et al., 1987). This suggests the purely GABAergic nature of such LDT elements.

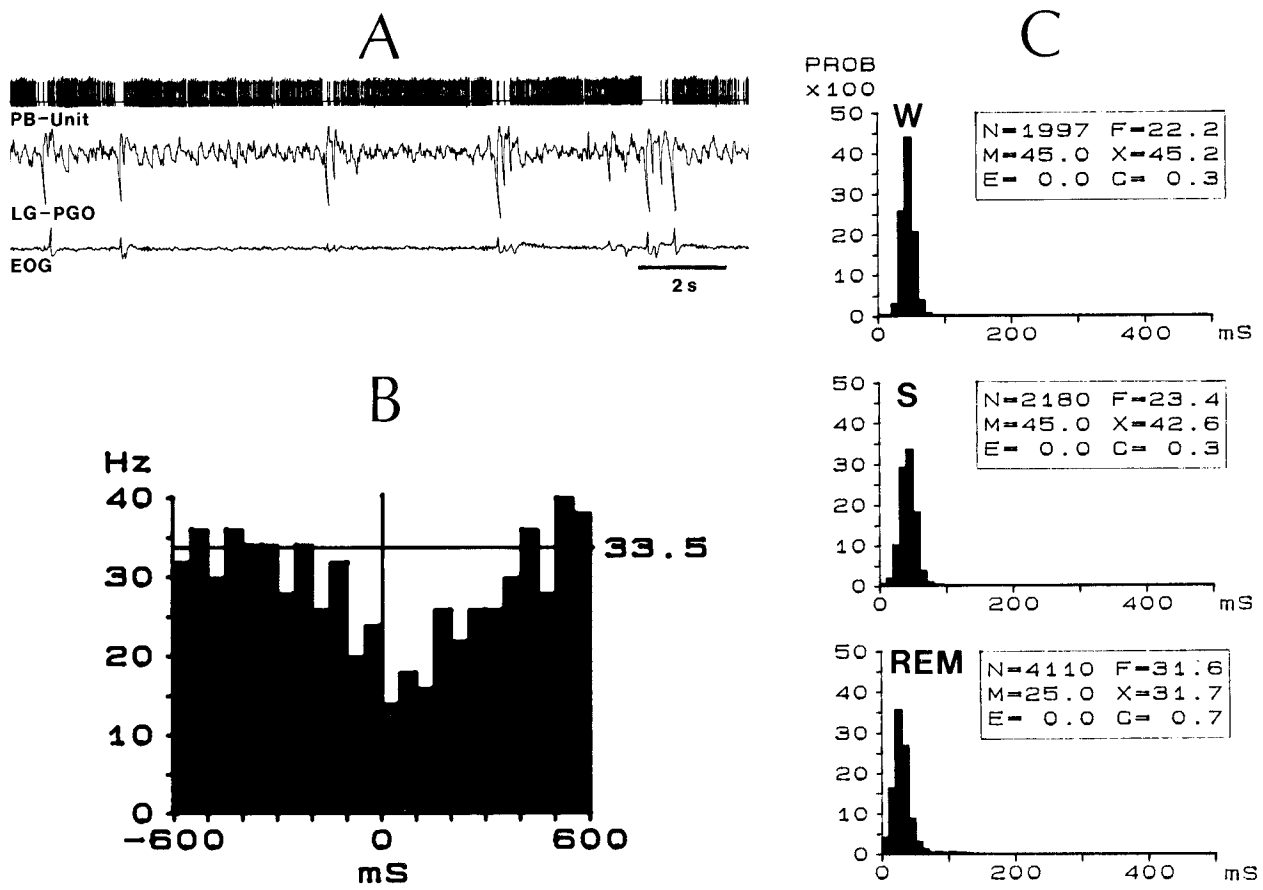

Figure 12. REM-on, PGO-off cell in the medial part of the PB area. *A,* Ink-written recording (unit activity, LG-PGO waves, and eye movements). *B,* PPSH with 50-msec bins. *C,* ISIHs of the same neuron during waking–sleep states (for symbols, see Figs. 4 and 8).

Assuming that PGO-off neurons are GABAergic, the arrest or striking diminution of their firing rates prior to and during PGO waves could disinhibit adjacent PGO-on neurons.

The PGO-off neurons may belong to the same family of inhibitory neurons as the eye-movement-related pause neurons located medially in the caudal pons (Ohgaki et al., 1987; Strassman et al., 1987), whose cessation of tonic firing acts to disinhibit premotor ocular neurons (Keller, 1977; Nakao et al., 1980).

Brain-stem reticular circuits involved in PGO genesis

In the following account, we consider that the bursting and tonic PGO-on PB/LDT neurons represent the final common path for the transfer of the PGO signal to the thalamus. Our study disclosed both short-lead (20–50 msec) and longer-lead (150 msec) PGO-on, thalamic-projecting neurons in mesopontine cholinergic nuclei. The presence of tonic PB/LDT neurons increasing their discharge rates about 150 msec before the LG-PGO wave does not, however, imply that PGO waves are exclusively generated within these nuclei. Previous studies have described neurons with lead times of 50–150 msec in the medial pontine reticular formation (McCarley and Ito, 1983). Also, some burst neurons of the medullary gigantocellular field, antidromically identified from the thalamus, were found to discharge selectively with LG-PGO waves (see phasic cell 1 in Fig. 6 of Steriade et al., 1984). Moreover, parallel experiments revealed that some tonic cells in the dorsal part of the midbrain central tegmental field are the longest-lead PGO-on elements. These neurons increase their discharge rates as much as 380 msec before thalamic PGO waves (Paré et al., 1990). All these data indicate that the brain-stem genesis of the PGO signal is attributable to a series of connected networks, from the medulla to the mesencephalon.

Figure 17 depicts the presumed synaptic interplay among different PGO-related cell types in PB/LDT nuclei and the possible influences they undergo from PGO-related neurons in other brain-stem reticular territories. Supporting morphological, electrophysiological, and pharmacological data have been mentioned above.

1. According to our hypothesis, sluggish-burst neurons are steadily inhibited by SNr GABAergic neurons. On that background of hyperpolarization, excitatory signals constituting corollary discharges of premotor ocular neurons trigger LTSs. We must, however, stress that excitatory drives from any part of the brain (the PB area receives a multitude of excitatory inputs, from the spinal cord, almost all brain-stem reticular territories, diencephalic areas, and cerebral cortex) could trigger LTSs. This is the reason why we emphasize that the content of PGO waves may well be mostly corollary information from eye-movement centers, as well as an event reflecting random impulses of central drives during REM sleep. For random impulses to generate a synchronized population event such as the PGO wave, we must postulate interconnections between cell types in mesopontine cholinergic nuclei (see the reciprocal loop between sluggish-burst and high-frequency burst neurons in Fig. 17, discussed in the following point).

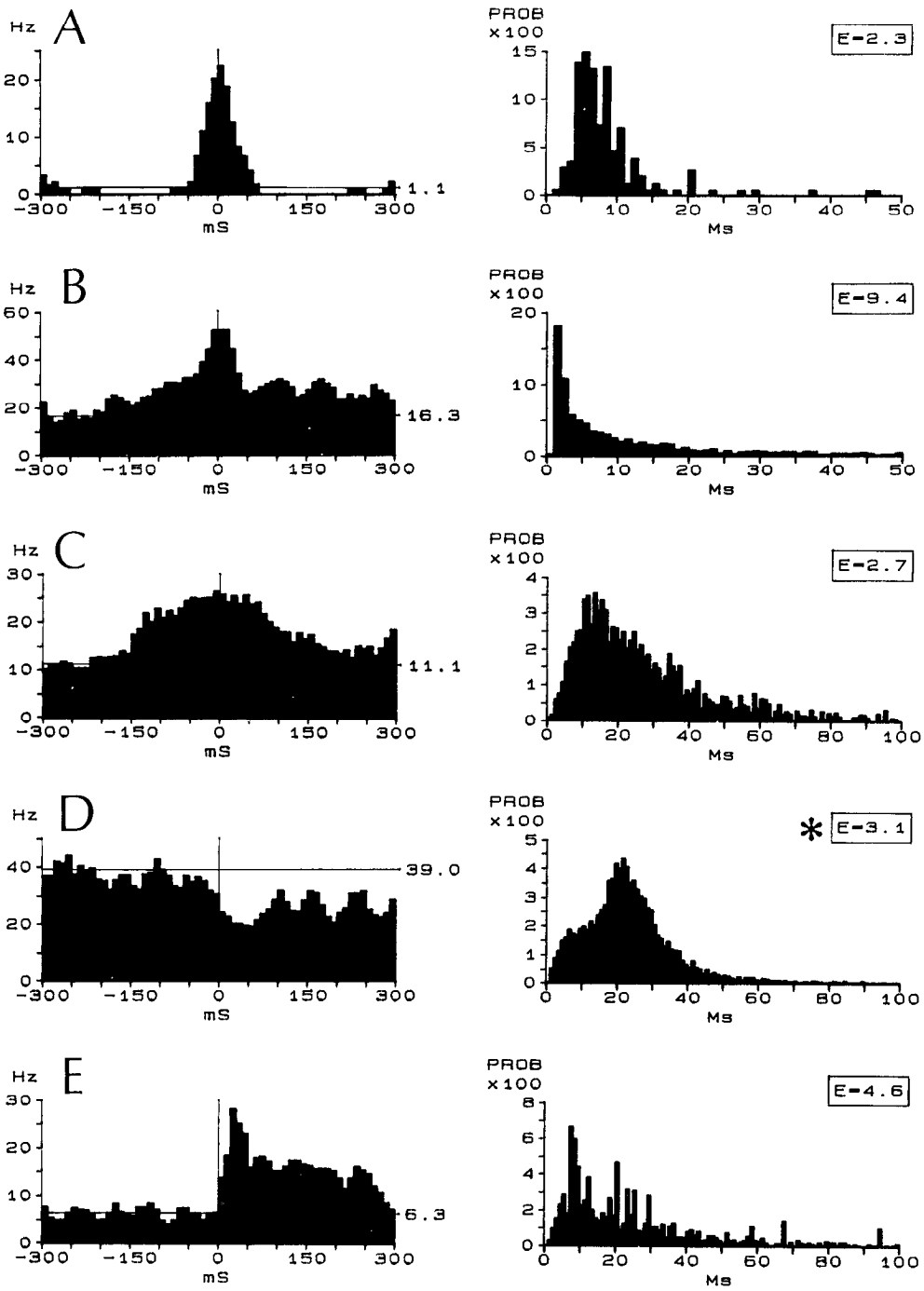

Figure 13. Analyses of PGO-related activity in pools of PGO-on sluggish-burst neurons (*A*, $n = 5$), PGO-on high-frequency burst neurons with tonically increased firing rates in REM sleep (*B*, $n = 11$), PGO-on tonic neurons (*C*, $n = 10$), REM-on but PGO-off neurons (*D*, $n = 3$), and post-PGO-on neurons (*E*, $n = 11$). PPSHs (*left column*) are depicted for all cellular types. PPIHs are depicted for *A–C* and *E* cellular types. Symbol *E* in PPIHs: percentage of PGO-related intervals in excess of the depicted time range. In *D*, *right column* (*asterisk*) depicts a pooled ISIH from REM sleep, instead of a PPIH, since the peri-PGO activity consists of a drop in firing rate.

2. High-frequency bursts are triggered by a prior acceleration of their spontaneous discharges. In turn, this acceleration is due to excitatory afferents from longer-lead PGO-on neurons found in the dorsal part of the central tegmental field and medial pontine reticular formation. It is proposed that these rostral midbrain and pontine reticular neurons use excitatory amino acids as transmitters. The progressive acceleration of discharges leads to a high-frequency burst at increased depolarized levels. High-frequency bursting PGO-on neurons excite PGO-on neurons with sluggish-bursts, and the latter reciprocate this action by feedback excitation of high-frequency burst neurons. This interconnection is suggested on the basis of ultrastructural studies showing that the dendrites of cat's pedunculopontine neurons are linked by means of complicated serial synapses (Moriizumi et al., 1989). Moreover, the hypothesized excitatory sign of this reciprocal connection between the 2 classes of bursting cells does not conflict with data showing that ACh induces hyperpolarizing effects upon PB/LDT neurons because sluggish-burst (LTS) neurons are not considered as cholinergic, and the hyperpolarizing effects of ACh (presumably released by both tonic and high-frequency burst cells) have not been described in LTS cells of the pedunculopontine nucleus.

3. PGO-on tonic neurons are driven by the same longer-lead neurons of brain-stem reticular territories outside the PB/LDT nuclei, as mentioned above (see point 2). The PGO-on tonic cells, presumably cholinergic, inhibit tonically discharging REM-

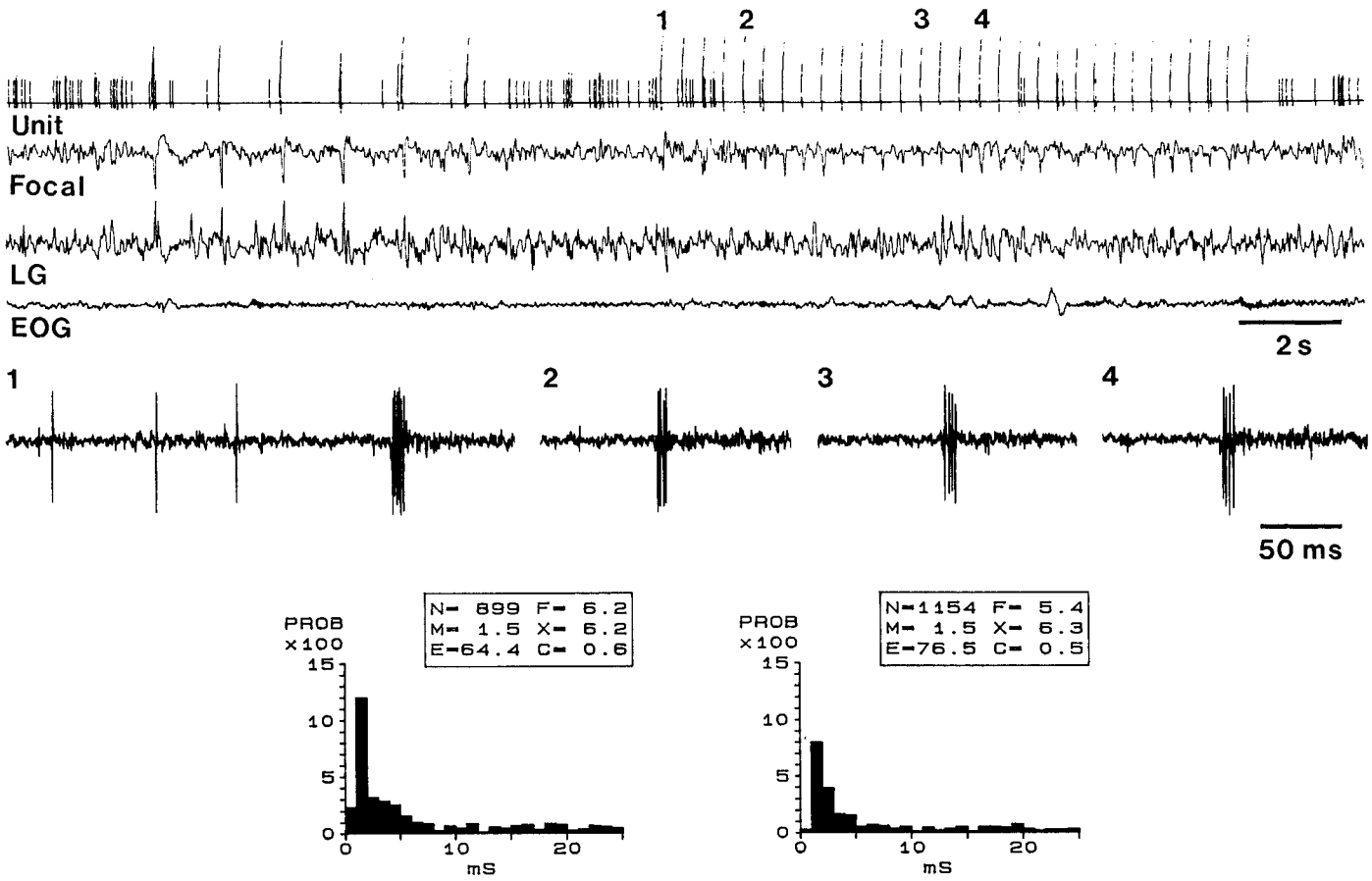

Figure 14. Sensory (hand-clapping)-induced PGO-like waves and high-frequency bursts in a PB neuron during W. The *top 4* ink-written traces depict unit activity (deflections exceeding the common level of single spikes represent high-frequency bursts), focal waves in PB area (recorded by the same microelectrode as used for action potentials), LG waves, and ocular movements. The portions indicated by numbers (*1–4*) on the ink-written *top trace* are also depicted with original spikes in oscilloscopic recordings. Below, ISIHs (1-msec bins) from 2 epochs of W, during which auditory stimuli were applied, to show the mode interval at 1.5 msec, reflecting the high intraburst frequency. For the polarity of LG waves (reversed as compared to LG-PGO waves during REM sleep), see text.

on PGO-off cells. In turn, the silenced firing of presumed GABAergic PGO-off cells leads to the disinhibition of PGO-on tonic neurons (and possibly of high-frequency burst cells), thus reinforcing their increased firing related to PGO waves (see the reciprocal image in Fig. 13, *C, D*). Note that the increased firing rate in tonic cells precedes by 150 msec the peak of PGO waves, while signs of decreased activity in PGO-off neurons are seen at about the same time in the averaged histogram (Fig. 13*D*) and much earlier (about 300 msec before the PGO wave) in the PPSH of the cell depicted in Figure 12*B*.

Possible functions of PGO waves

The hypothesis was proposed that EMPs during W, as well as PGO waves during REM sleep, are central correlates of orienting reactions (Bowker and Morrison, 1976). This is consistent with the fact that, if muscular atonia is suppressed by adequate pontine lesions, animals display typical orienting and searching behaviors during episodes of bona fide REM sleep (Jouvet and Delorme, 1965), as if they were responding to internally generated signals. A similar hallucinatory syndrome can be observed during the W state, in the early excitatory phase induced by microinjections of glutamate analogs into the mesopontine PB area (Kitsikis and Steriade, 1981). The hypothesis that EMPs and PGO waves are orienting reactions to stimuli from the outside world or to internal drives is supported by the habituation of these responses (Bowker and Morrison, 1976; Ball et al., 1989).

We have shown that (1) spiky field potentials (with a morphology identical to that of EMPs and PGO waves) evoked in the PB area by hand-clapping are associated with spike bursts of PB neurons; (2) habituation of these mass and unit events during W does occur much more readily in the thalamus than the brain-stem (Figs. 14, 15); (3) "orienting" PB burst neurons may also respond during REM sleep (Fig. 16); and (4) although some PB neurons discharging spike bursts in response to sensory stimuli during W do also fire in phase with spontaneous brain-stem PGO waves during REM sleep (Fig. 16*B*), other neurons are not related with PGO waves (Fig. 15*A*). These data show that there is no blockade at the peripheral gates (intra-auricular muscle contraction and centrifugal inhibition of cochlear nucleus) preventing PB and thalamic neurons to be driven by strong sensory stimuli during either W or REM sleep. That the brain-stem PB area is open to external stimuli during REM sleep, whereas thalamic nuclei apparently do not respond to the same sensory stimuli (Fig. 16*A*), is unexpected in view of the demonstration that thalamic neurons are highly responsive to central stimuli during REM sleep (Steriade, 1984). Since LG-PGO waves induced by auditory stimulation display great la-

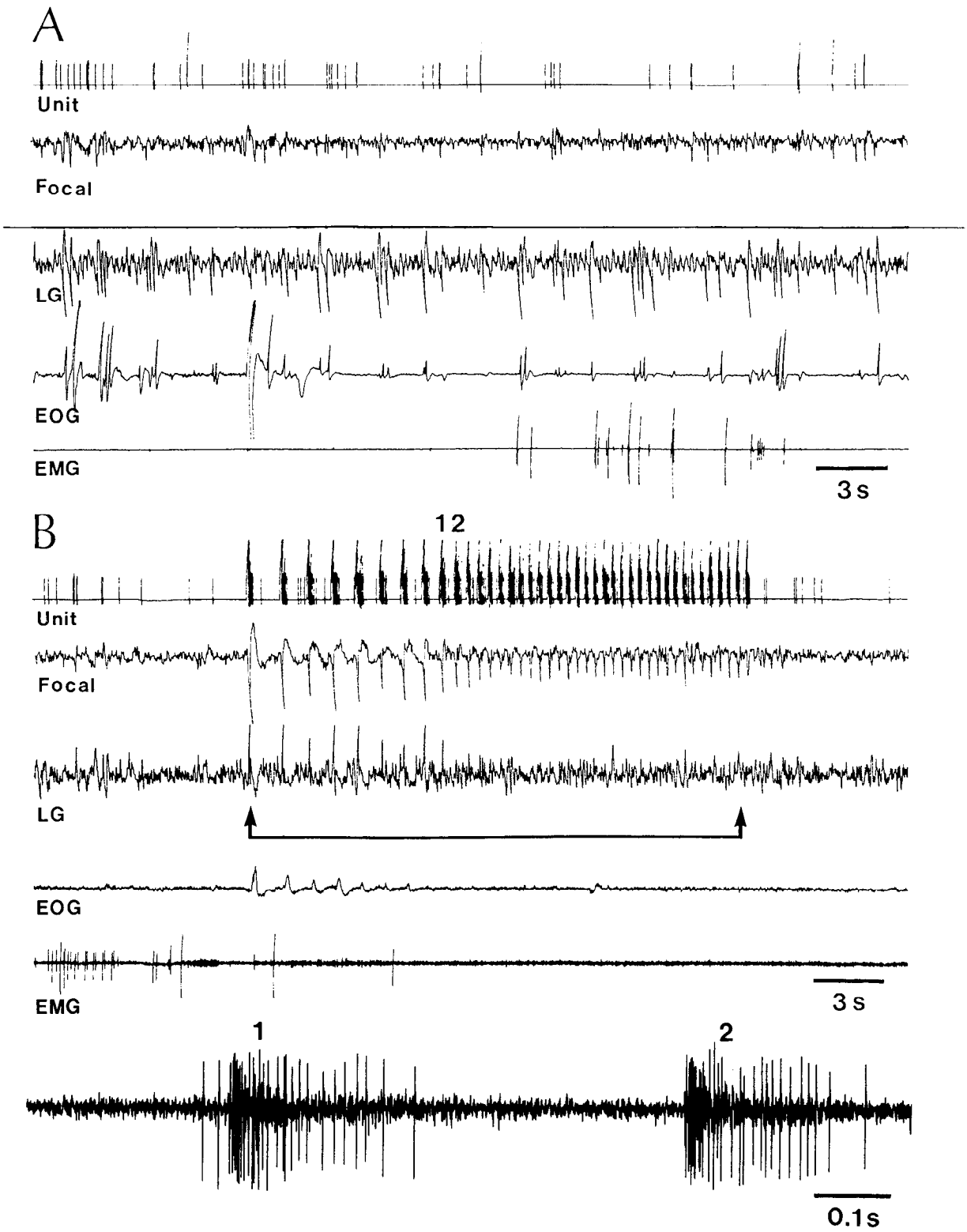

Figure 15. Sensory (hand-clapping)-induced PGO-like waves and high-frequency bursts in a PB neuron during W. *A*, Polygraphic recording during REM sleep; same as in Figure 14, with an additional electromyographic trace. Note absence of relations between PB-cell's discharges and LG-PGO waves. *B*, Same type of polygraphic recording as above, showing the effect of 1/sec and then 2/sec hand-clapping during W (*between arrows*). Note diminution in amplitude of PGO-like waves in PB area and disappearance of eye movements, as well as corresponding LG waves, by increasing the rate of sensory stimulation. Spike bursts indicated on *top* ink-written trace (*1, 2*) are also depicted with original spikes in the *bottom* oscilloscopic record. Note also the reversed polarity of auditory-induced LG waves in W, as compared with LG-PGO waves in REM sleep (see text).

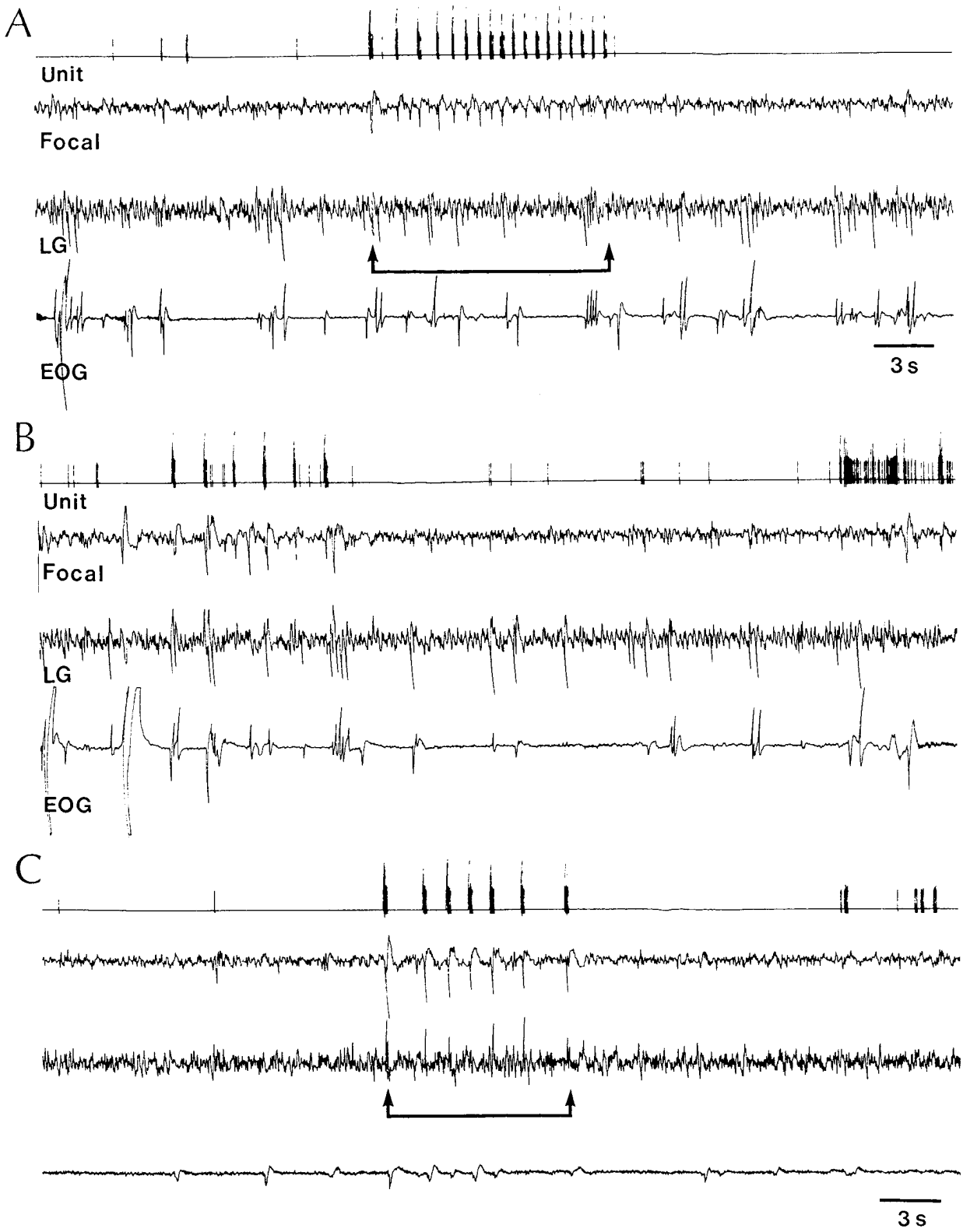

Figure 16. Sensory (hand-clapping)-induced PGO-like waves in PB area, associated with high-frequency bursts in a PB cell, during both REM sleep and W. Neuron antidromically activated from the thalamic LG nucleus. Traces in polygraphic recordings similar to those in Figures 14 and 15. *A,* Activity evoked by auditory stimuli (*between arrows*) during REM sleep. *B,* Spontaneous spike bursts of PB cell, related to focal PGO waves in the PB area, during REM sleep. *C,* Activity evoked by auditory stimuli (*between arrows*) during W.

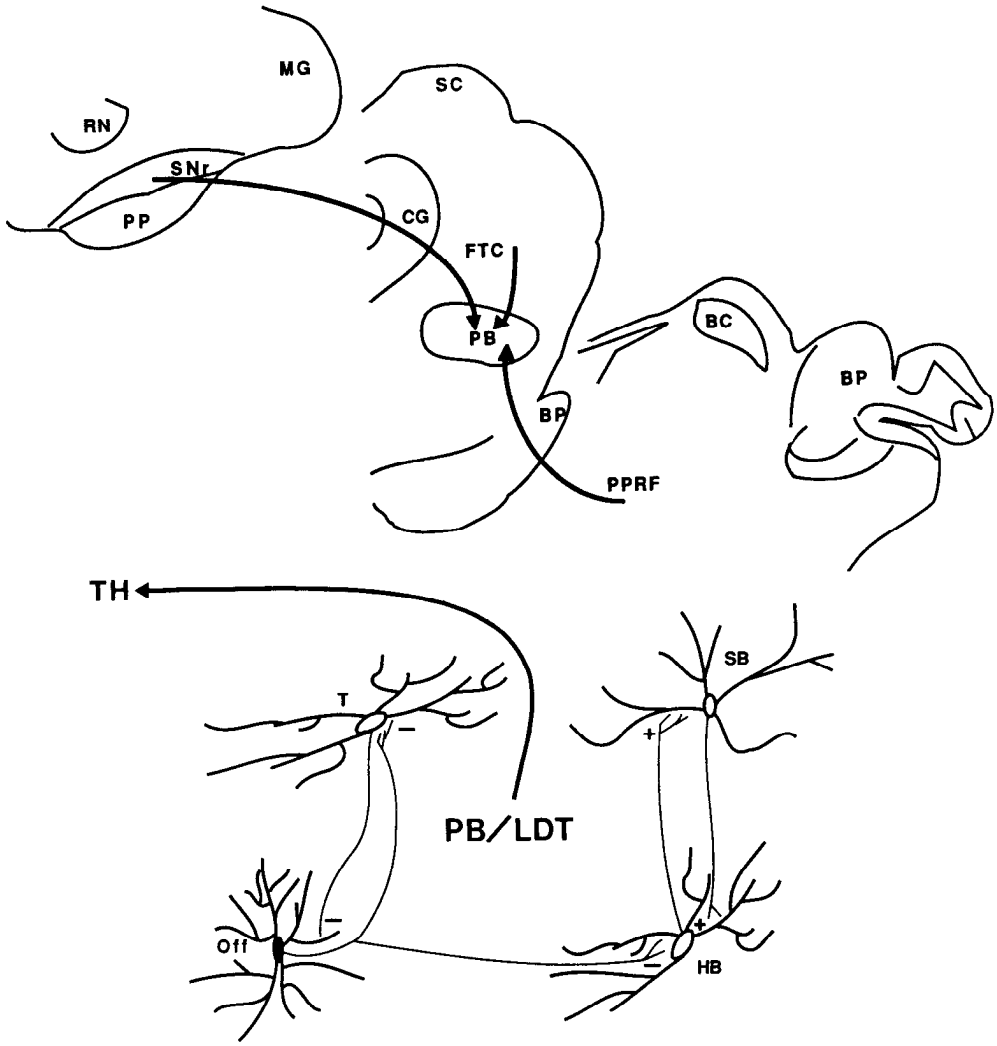

Figure 17. Tentative schemes of cellular interactions underlying the genesis of PGO waves and their transfer from PB/LDT nuclei to the thalamus (*TH*). *Top,* Three frontal sections (from rostral to caudal) depicting the inputs to PB area from substantia nigra pars reticulata (*SNr*), central tegmental field (*FTC*), and the paramedian pontine reticular formation (*PPRF*). Other abbreviations: *BC,* brachium conjunctivum; *BP,* brachium pontis; *CG,* central gray; *MG,* medial geniculate nucleus; *PP,* pes pedunculi; *RN,* red nucleus; *SC,* superior colliculus. *Bottom,* Hypothesized excitatory (+) and inhibitory (−) interactions between 4 cellular types (PGO-on and PGO-off) in PB/LDT nuclei. Symbols (*SB, HB, Off, T*) as in Figure 1; see also explanations in text.

tency variation during REM sleep (Wu et al., 1989), spontaneously occurring PGO waves may be limiting factors for the appearance of sensory-evoked responses.

The PGO signal generated in the brain stem activates thalamocortical neurons through 2 types of cholinergic events: a rapid nicotinic excitation (McCormick and Prince, 1987), responsible for the phasic depolarization associated with the LG-PGO wave (Hu et al., 1989); and a slow muscarinic depolarization (McCormick and Prince, 1987) that is reflected in the relatively long trains of action potentials which follow the initial excitation during LG-PGO waves (Steriade et al., 1989). These processes at the level of the thalamic visual nucleus are likely concomitant to similar events in many other cortical-projecting thalamic nuclei because PGO waves largely transcend the geniculostriate system. In turn, the PGO-related thalamic processes induce excitatory effects upon cortical target cells. The absence of PGO waves would then reduce internally generated activation processes in thalamocortical systems. Indeed, suppression of LG-PGO waves by bilateral lesions of the brainstem PB areas results in an increased latency of the LG-cell response to optic chiasm stimulation, a reduced proportion of X-type cells compared to age-paired controls, and a smaller LG somata (Davenne et al., 1989). These data provide support for the ontogenetic hypothesis (Roffwarg et al., 1966) that endogenous PGO activity is necessary for the correct expression of some innate program and plays a major role in structural maturation, especially during the period of early infancy when REM epochs occupy most of the sleep time.

References

Beckstead RM (1982) Long collateral branches of substantia nigra pars reticulata axons to thalamus, superior colliculus and reticular formation in monkey and cat. Multiple retrograde neuronal labeling with fluorescent dyes. Neuroscience 10:767–779.

Beckstead RM, Frankfurter A (1982) The distribution and some morphological features of substantia nigra neurons that project to the thalamus, superior colliculus and pedunculopontine nucleus in the monkey. Neuroscience 10:2377–2388.

Ball WA, Morrison AR, Ross RJ (1989) The effects of tones on PGO waves in slow wave sleep and paradoxical sleep. Exp Neurol 104: 251–256.

Bowker RM, Morrison AR (1976) The startle reflex and PGO spikes. Brain Res 102:185–190.

Callaway CW, Lydic R, Baghdoyan HA, Hobson JA (1987) Pontogeniculooccipital waves: spontaneous visual system activity during rapid eye movement sleep. Cell Mol Neurobiol 7:105–149.

Celio MR (1986) Parvalbumin in most gamma-aminobutyric acid-containing neurons of the rat cerebral cortex. Science 231:995–997.

Celio MR, Heizmann CW (1981) Calcium-binding protein parvalbumin as a neuronal marker. Nature 293:300–302.

Christie MJ, North RA (1988) Agonists at μ-opioid, M_2-muscarinic

and $GABA_B$-receptors increase the same potassium conductance in rat lateral parabrachial neurones. Br J Pharmacol 95:896–902.
Coulter DA, Huegenard JR, Prince DA (1989) Calcium currents in rat thalamocortical relay neurones: kinetic properties of the transient, low-threshold current. J Physiol (Lond) 414:587–604.
Datta S, Curró Dossi R, Paré D, Oakson G, Steriade M (1990) Discharges of substantia nigra reticulata (SNR) neurons during sleep-waking states. Soc Neurosci Abstr 16 (in press).
Davenne D, Frégnac Y, Imbert M, Adrien J (1989) Lesion of the PGO pathways in the kitten. II. Impairment of physiological and morphological maturation of the lateral geniculate nucleus. Brain Res 485: 267–277.
Deniau JM, Hammond C, Féger J, Albe-Fessard D (1979) Substantia nigra efferent connections. Appl Neurophysiol 42:65–68.
Eccles JC, Ito M, Szentágothai J (1967) The cerebellum as a neuronal machine. New York: Springer.
Egan TM, North RA (1986) Acetylcholine hyperpolarizes central neurones by acting on an M_2 muscarinic receptor. Nature 319:405–407.
El Mansari M, Sakai K, Jouvet M (1989) Unitary characteristics of presumptive cholinergic tegmental neurons during the sleep-waking cycle in freely moving cats. Exp Brain Res 76:519–529.
Gerber U, Greene RW, McCarley RW (1989) Repetitive firing of medial pontine reticular formation neurones of the rat recorded *in vitro*. J Physiol (Lond) 410:533–560.
Hikosaka O, Wurtz RH (1983) Visual and oculomotor functions of monkey substantia nigra pars reticulata. I. Relation of visual and auditory responses to saccades. J Neurophysiol 49:1230–1253.
Hu B, Bouhassira D, Steriade M, Deschênes M (1988) The blockage of ponto-geniculo-occipital waves in the cat lateral geniculate nucleus by nicotinic antagonists. Brain Res 473:394–397.
Hu B, Steriade M, Deschênes M (1989) The cellular mechanism of thalamic ponto-geniculo-occipital waves. Neuroscience 31:25–35.
Jourdain A, Semba K, Fibiger HC (1989) Basal forebrain and mesopontine tegmental projections to the reticular thalamic nucleus: an axonal collateralization and immunohistochemical study in the rat. Brain Res 505:55–65.
Jouvet M, Delorme JF (1965) Locus coeruleus et sommeil paradoxal. CR Soc Biol (Paris) 159:895–899.
Kang Y, Kitai ST (1990) Electrophysiological properties of pedunculopontine neurons and their postsynaptic responses following stimulation of substantia nigra reticulata. Brain Res (in press).
Keller EL (1977) Control of saccadic eye movements by midline brain stem neurons. In: Developments in neuroscience, Vol 1: control of gaze by brain stem neurons (Baker R, Berthoz A, eds), pp 327–336. Amsterdam: Elsevier.
Kitsikis A, Steriade M (1981) Immediate behavioral effects of kainic acid injections into the midbrain reticular core. Behav Brain Res 3: 361–380.
Kosaka T, Kosaka K, Hataguchi Y, Nagatsu I, Wu JY, Ottersen OP, Storm-Mathisen J, Hama K (1987) Catecholaminergic neurons containing GABA-like and/or glutamic acid decarboxylase-like immunoreactivities in various brain regions of the rat. Exp Brain Res 66: 191–210.
Leonard CS, Llinás R (1987) Low-threshold calcium conductance in parabrachial reticular neurons studied *in vitro* and its blockade by octanol. Soc Neurosci Abstr 13:1012.
Leonard CS, Llinás R (1988) Electrophysiology of thalamic-projecting brainstem neurons and their inhibition by ACh. Soc Neurosci Abstr 14:297.
Leonard CS, Llinás RR (1990) Electrophysiology of mammalian pedunculopontine and laterodorsal tegmental neurons *in vitro*: implications for the control of REM sleep. In: Brain cholinergic systems (Steriade M, Biesold D, eds), pp 205–223. New York: Oxford UP.
McCarley RW, Ito K (1983) Intracellular evidence linking medial pontine reticular formation neurons to PGO wave generation. Brain Res 280:343–348.
McCarley RW, Nelson JP, Hobson JA (1978) Ponto-geniculo-occipital (PGO) burst neurons: correlative evidence for neuronal generators of PGO waves. Science 201:269–272.
McCormick DA, Prince DA (1987) Actions of acetylcholine in the guinea pig and cat medial and lateral geniculate nuclei, *in vitro*. J Physiol (Lond) 392:147–165.
Moriizumi T, Nakamura Y, Tokuno H, Kudo M, Kitao Y (1989) Synaptic organization of the pedunculopontine tegmental nucleus of the cat. Brain Res 478:315–325.
Nakao S, Curthoys IS, Markham CH (1980) Direct inhibitory projection of pause neurons to nystagmus-related pontomedullary reticular burst neurons in the cat. Exp Brain Res 40:283–293.
Nelson JP, McCarley RW, Hobson JA (1983) REM sleep burst neurons, PGO waves, and eye movement information. J Neurophysiol 50:784–797.
Ohgaki T, Curthoys IS, Markham CH (1987) Anatomy of physiologically identified eye-movement-related pause neurons in the cat: pontomedullary region. J Comp Neurol 266:56–72.
Paré D, Curró Dossi R, Datta S, Steriade M (1990) Brainstem genesis of reserpine-induced ponto-geniculo-occipital waves: an electrophysiological and morphological investigation. Exp Brain Res (in press).
Roffwarg HP, Muzio JN, Dement WC (1966) Ontogenic development of the human sleep-dream cycle. Science 152:604–619.
Ruch-Monachon, MA, Jaffre M, Haefely W (1976) Drugs and PGO waves in the lateral geniculate body of the curarized cat. IV. The effects of acetylcholine, GABA and benzodiazepines on PGO wave activity. Arch Int Pharmacodyn Ther 219:308–325.
Saito H, Sakai K, Jouvet M (1977) Discharge patterns of the nucleus parabrachialis lateralis neurons of the cat during sleep and waking. Brain Res 134:59–72.
Sakai K (1985) Anatomical and physiological basis of paradoxical sleep. In: Brain mechanisms of sleep (McGinty DJ, Drucker-Colin R, Morrison A, Parmeggiani RL, eds), pp 111–137. New York: Raven.
Sakai K, Jouvet M (1980) Brain stem PGO-on cells projecting directly to the cat dorsal lateral geniculate nucleus. Brain Res 194:500–505.
Sakai K, Petitjean F, Jouvet M (1976) Effects of ponto-mesencephalic lesions and electrical stimulation upon PGO waves and EMPs in unanesthetized cats. Electroenceph Clin Neurophysiol 41:49–63.
Scarnati E, Proia A, DiLoreto S, Pacitti C (1987) The reciprocal electrophysiological influence between the nucleus tegmenti pedunculopontinus and the substantia nigra in normal and decorticated rats. Brain Res 423:116–124.
Steriade M (1984) The excitatory-inhibitory response sequence in thalamic and neocortical cells: state-related changes and regulatory systems. In: Dynamic aspects of neocortical function (Edelman GM, Gall WE, Cowan WM, eds), pp 107–157. New York: Wiley-Interscience.
Steriade M, Llinás RR (1988) The functional states of the thalamus and the associated neuronal interplay. Physiol Rev 68:649–742.
Steriade M, McCarley RW (1990) Brainstem control of wakefulness and sleep. New York: Plenum.
Steriade M, Paré D (1990) Brainstem genesis and thalamic transfer of ponto-geniculo-occipital waves: cellular data and hypotheses. In: Sleep and biological rhythms (Montplaisir J, Godbout R, eds), pp 148–162. New York: Oxford UP.
Steriade M, Sakai K, Jouvet M (1984) Bulbo-thalamic neurons related to thalamocortical activation processes during paradoxical sleep. Exp Brain Res 54:463–475.
Steriade M, Domich L, Oakson G (1986) Reticularis thalamic neurons revisited: activity changes during shifts in states of vigilance. J Neurosci 6:68–81.
Steriade M, Paré D, Bouhassira D, Deschênes M, Oakson G (1989) Phasic activation of lateral geniculate and perigeniculate thalamic neurons during sleep with ponto-geniculo-occipital waves. J Neurosci 9:2215–2229.
Steriade M, Datta S, Paré D, Oakson G, Curro Dossi R (1990) Neuronal activities in brain-stem cholinergic nuclei related to tonic activation processes in thalamocortical systems. J Neurosci 10:2541–2559.
Strassman A, Evinger C, McCrea RA, Baker RG, Highstein SM (1987) Anatomy and physiology of intracellularly labelled omnipause neurons in the cat and squirrel monkey. Exp Brain Res 67:436–440.
Wainer BH, Mesulam M-M (1990) Ascending cholinergic pathways in the rat brain. In: Brain cholinergic systems (Steriade M, Biesold D, eds, pp 65–119). New York: Oxford UP.
Webster HH, Jones BE (1988) Neurotoxic lesions of the dorsolateral pontomesencephalic tegmentum-cholinergic cell area in the cat. II. Effects upon sleep-waking states. Brain Res 458:285–302.
Wilcox KS, Grant SJ, Burkhart BA, Cristoph GR (1989) *In vitro* electrophysiology of neurons in the lateral dorsal tegmental nucleus. Brain Res Bull 22:557–560.
Wu MF, Mallick BN, Siegel JE (1989) Lateral geniculate spikes, muscle atonia and startle response elicited by auditory stimuli as a function of stimulus parameters and arousal state. Brain Res 499:7–17.